ENGINEERING DEVELOPMENT ANALYSIS OF A SEGMENTED PROJECTILE SABOT

FINAL REPORT

PREPARED FOR

* DEFENCE R&D CANADA – VALCARTIER
R&D POUR LA DÉFENSE CANADA - VALCARTIER
QUEBEC, QC G3J 1X5
CANADA
Contract No.: W7701-3-4635/001/QCA
Guy Bergeron, Scientific authority
Tel: 418-844-4000 ext. 4443

By

É. Bélanger
G. Bergeron*
P.Gosselin

NUMERICA TECHNOLOGIES INC.
3420 rue Lacoste
Québec, QC G2E 4P8 Canada

March 2005

TABLE OF CONTENTS

LIST OF FIGURES

LIST OF TABLES

1.0 INTRODUCTION

Studies in regard of penetration show that for an equivalent weight in hyper velocity condition, some small penetrators with gap are more efficient in term of penetration than a penetrator alone. To demonstrate this theory in experimentation, the same test must be done at Mach 6.7 for the monolithic and the segmented projectile concepts. The segmented projectile is analysed for two different designs: the conceptual and the engineering. All the characteristics of the projectile in regard of components description, assembly weight and core weight must be the same. Experimental acceleration equipment and adequate instrumentation are necessary to control data and projectile behaviour in term of ballistic aspects.

The launch of these two projectiles in the light gas gun needs the presence of a sabot. A sabot allows a projectile of a smaller calibre to be fired within a larger-bore accelerator. The sabot fills the bore of the gun during the firing stage. Usually, the sabot is a lightweight carrier. This means, the sabot's effect on the core mass must be minimal during the impact with the target.

This report will put some attention on the sabot resistance and on its capability to survive the loading conditions inside the light gas gun caused by the acceleration during the launch. This report will show the main results of the development for the sabot/projectile assembly. All the permitted dimensions and materials will be experimented to get a final sabot assembly that can resist to the pressure during the firing stage. Some analytical calculation will be done to give some orientation before numerical simulations. Numerical simulations and preliminary compression tests in static will also verify all the design aspects.

2.0 BACKGROUND AND CONSIDERATIONS

2.1 DESIGN TYPE

2.1.1 MONOLITHIC DESIGN

Figure 1 shows the monolithic preliminary design representation. The white part represents the sabot in term of preliminary design. The sabot is supposed to be in polycarbonate. The blue part represents the projectile in one part. The projectile is in tungsten alloy. The sabot and the monolithic tungsten projectile will be defined as the monolithic launch package.

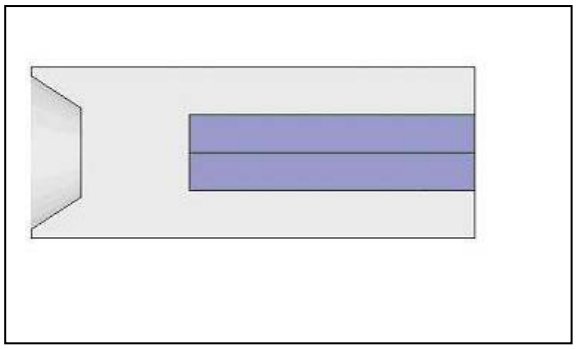

Figure 1 – Monolithic preliminary design representation

2.1.2 SEGMENTED DESIGN

Figure 2 shows the segmented preliminary design representation. The white part represents the sabot in term of preliminary design. The sabot is supposed to be in polycarbonate. The grey part represents the spacer between the segments. The spacers are also in polycarbonate. The blue parts represent the segments of the projectile. The projectile is in tungsten alloy. The sabot, the spacers and the tungsten segments will be defined as the segmented launch package for this report. The term launch package will be used in general to describe the global assembly of the sabot components and the tungsten projectile.

Figure 2 – Segmented preliminary design representation

2.2 ANALYSIS TYPE

This section presents all the analysis completed during the analysis process to achieve a sabot design that resist the loading of the pressure inside the gas gun. These analysis are analytic, static and transient.

2.2.1 ANALYTIC CALCULATION

Figure 3 shows the area considered for the analytic calculation. Particularly, the oval shows the shear area in the rear part of the sabot. This analysis permits the evaluation of the preliminary minimum shear area the sabot must have to resist to the back face pressure. This evaluation helps to supply preliminary dimensions of the sabot before any software simulation begins. Analytic analyses are developed in section 3.1.

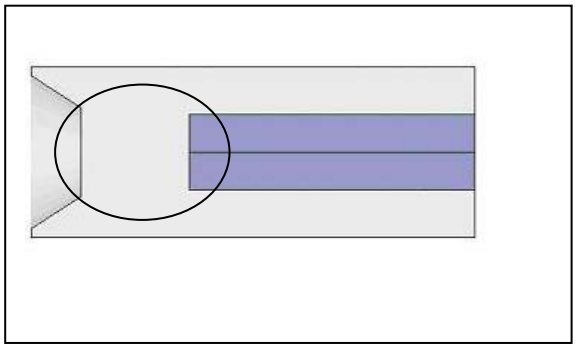

Figure 3 – Area considered in the analytic

2.2.2 NUMERICAL SIMULATION INFORMATION

All the models for the analysis were prepared in the 2D modeling section of ANSYS ® a Finite Element Analysis (FEA) software. All numerical simulations were solved by ANSYS ® also. This FEA software permits static and transient analysis. Due to the axisymmetric nature of the problem, a 2D model was analysed to greatly reduce the amount of elements and solving resources.

2.2.3 STATIC NUMERICAL SIMULATION

Figure 4 shows the loading and the boundary conditions on the sabot for the static analysis simulation. This figure shows a 2-dimensionnal view of the half sabot for an axisymmetric view. The blue part represents the sabot, the purple part represents the spacer and the cyan part represents the projectile.

The red arrows on the right represent the backpressure distribution on the sabot. The blue triangles on the top and the bottom represent movement constraints to $\Delta x = 0$ in the x-axis. The triangles on the left represent a movement constraint to $\Delta y = 0$ in the

y-axis. During the simulation, the pressure pushes the sabot toward left, but the resistance comes from the locking position of the projectile in the y-axis which represent the effect of projectile inertia. During that type of simulation, the stress and deformation of the sabot will be more important than in real life because only 50 % of the sidewall sabot inertia has been considered. This was aimed at ensuring a worst-case scenario with regard to shear stress. The black arrow on the left represent this part of the sabot inertia plus the front pressure of sabot during the acceleration process.

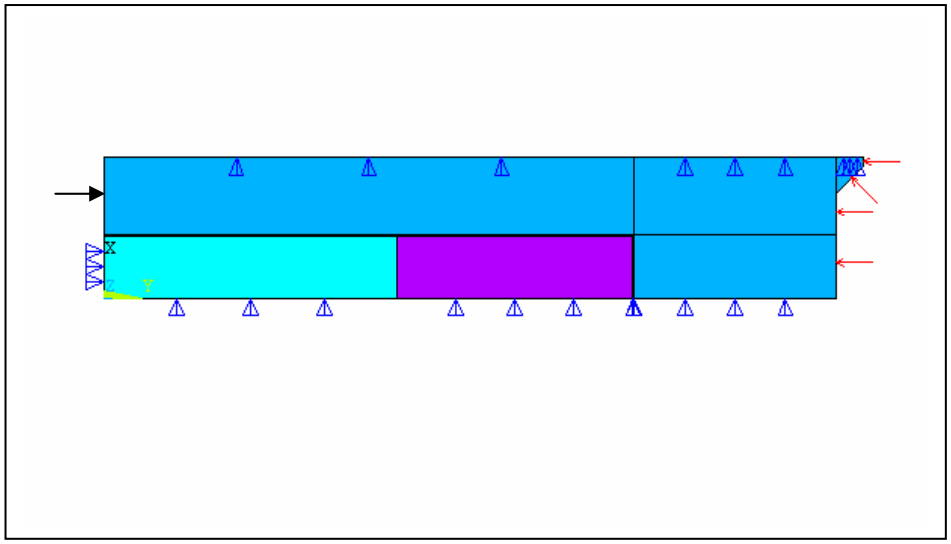

Figure 4 – Loading and boundary conditions for the static analysis simulation

Figures 5 and 6 show the curves used to evaluate the pressure value applied to the sabot. Figure 5 gives the backpressure applied to the sabot in function of time and Figure 6 gives the front pressure applied to the sabot in function of time. These curves come from the IGG3 code for the gas gun simulation from the University of Toronto. Figure 6 shows different points on curve. Points 14 and 18 represent the maximum backpressure with a value of around 207 MPa. The backpressure value of 200 MPa has been considered for the analytic calculation and static simulation.

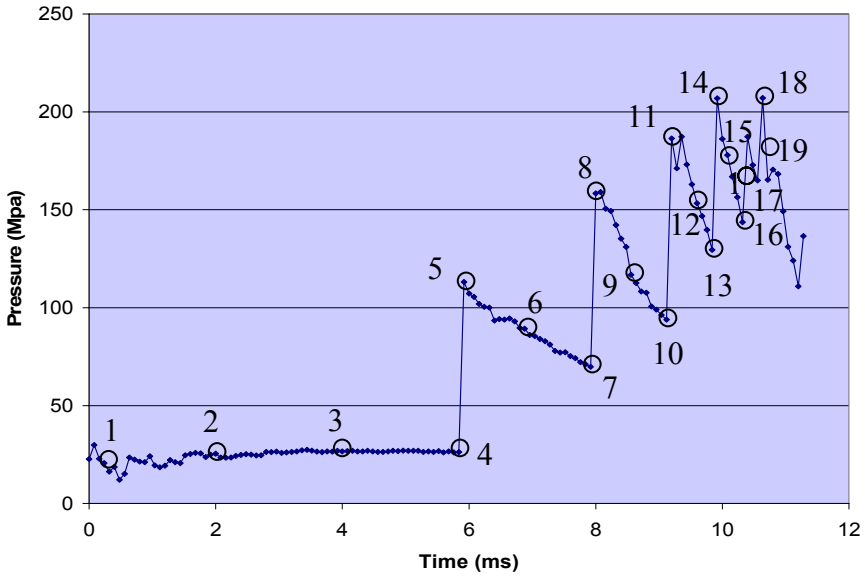

Figure 5 – Backpressure applied to the sabot from the IGG3 code

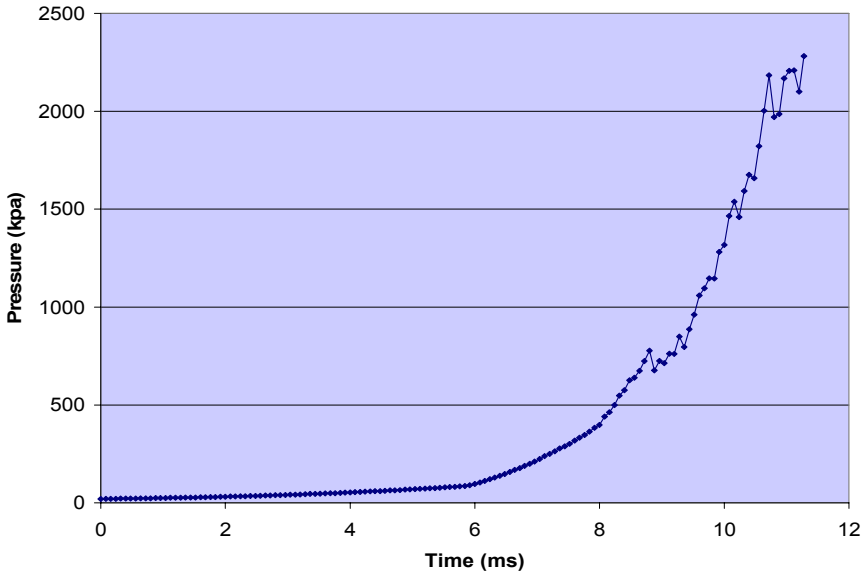

Figure 6 – Front pressure applied to the sabot from the IGG3 code

2.2.4 CRITERIA FOR SIMULATION EVALUATION

The evaluation of the ability of the sabot to survive the launch is done by some criteria analysis. In fact, the stress in the x-axis, xy-axis and y-axis are particularly interesting because they bring answers to the resistance for the radial, the shear and the compression stress. All the results of the design have been considered and evaluated for the stress in these three axis.

2.3 MATERIAL PROPERTIES

Table 1 shows the material properties for all the materials used in the launch package: tungsten alloy 490S, polycarbonate Lexan and polyetherimide Ultem 1000 All the properties of this table were necessary to achieve a design with the simulation analysis on software. More details about the properties are available in appendix A.

Table 1 – Material properties

Material	Tungsten	Polycarbonate	Ultem *
Density (g/cm^3)	17.15	1.20	1.28
Shear Strength (MPa)	N.A.	63.4	103.4
Tensile Strength (MPa)	1 472	72.4	113.8
Compressive Strength (MPa)	N.A.	79.3	151.7
Young Modulus (MPa)	275 000	2 413	3 447
Poisson's Ratio	0.334	0.4	0.36

* The polyetherimide Ultem listed in this text is the material Ultem grade 1000. By now, to simplify the text, only the term Ultem will be used to represent the Ultem 1000.

2.4 DESIGN CRITERIA

Table 2 presents the design criteria that the sabot assembly must have to be considered as a success in term of design. The criteria are in terms of dimensions, weight, components, resistance and material.

Table 2 – Design criteria for the sabot and components

Descriptions	Values
Maximum sabot diameter	49.6 mm
Diameter of tungsten and polycarbonate segment	22 mm
Length of tungsten and polycarbonate segment	10.5 mm
Total launch package weight	700 g
Weight loss by projectile edge radius	Maximum 10 %
Number of segments in the projectile	Minimum of 5 segments
Maximum backpressure on the sabot	200 MPa
Sabot material	Unfilled Polycarbonate

3.0 PRELIMINARY SABOT ANALYSIS RESULTS

3.1 ANALYTIC CALCULATION RESULTS

3.1.1 SHEAR STRENGTH EVALUATION

The following equation gives the value of the maximum shear stress independent of the shape for the parts involved. That value permitted to know the minimal area value for the preliminary shear analysis.

$$Sc = \frac{P \cdot (D^2 - d^2)}{4 \cdot d \cdot L} \tag{3.1}$$

As mentioned in table 1, the admissible stress value in shear is 63.4 MPa for the polycarbonate. Figure 7 gives the detailed dimensions to calculate the shear area on the sabot.

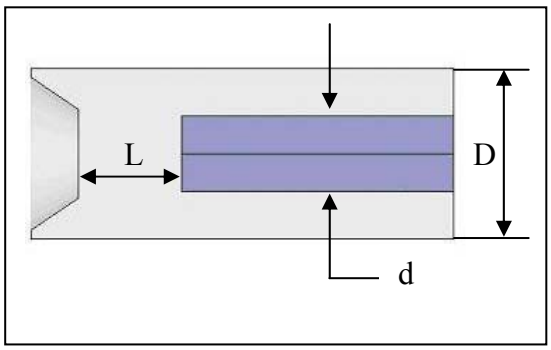

Figure 7 – Dimensions to calculate shear area on the sabot

With equation 3.1, the maximum shear stress in the polycarbonate is 124.75 MPa. This value is true if the considered length in the rear part of the projectile is 36 mm (L) and the backpressure is 200 MPa (P). Because the maximum shear stress exceeds the admissible shear stress of the polycarbonate, the sabot will fail for the dimensions previously presented. These dimensions come from concept 1. Even if the sabot fails in this example, the concept 1 will be described with more details and numerically analysed nevertheless in Section 3.2 to validate the model in ANSYS ®.

3.1.2 ACCELERATION DIFFERENCE FOR SABOT AND PROJECTILE

The following equation gives the value of the acceleration for the components involved in the sabot in function of the pressure. That value allowed comparing the acceleration difference between the lightweight sabot and the projectile.

$$a = \frac{P \cdot A}{M} \tag{3.2}$$

Where P is the pressure on the sabot
A is the area where the pressure is applied
M is the mass accelerated

With equation (3.2), the lightweight sabot acceleration is 8.7E6 m/s^2 while the projectile acceleration is 4.1E6 m/s^2 if the dimensions of concept 4 are taken. This validation allowed realising the amplitude of the shear strength necessary to compensate the acceleration mismatch. Many details about the concept 4 are available in the section 3.2.4.

3.2 STATIC NUMERICAL SIMULATION RESULTS

Even though the first concepts of sabot were assessed by analytical calculation, they were formally evaluated by static numerical simulation.

3.2.1 CONCEPT 1 - POLYCARBONATE EXTERNAL SHELL ONLY

Physical description and dimension details

This concept is equivalent to the design types presented in section 2.1. Figure 8 shows the numerical modeling layout of concept 1 assembly. The cyan, purple and blue colours represent respectively the tungsten projectile, the polycarbonate spacer and the polycarbonate sabot.

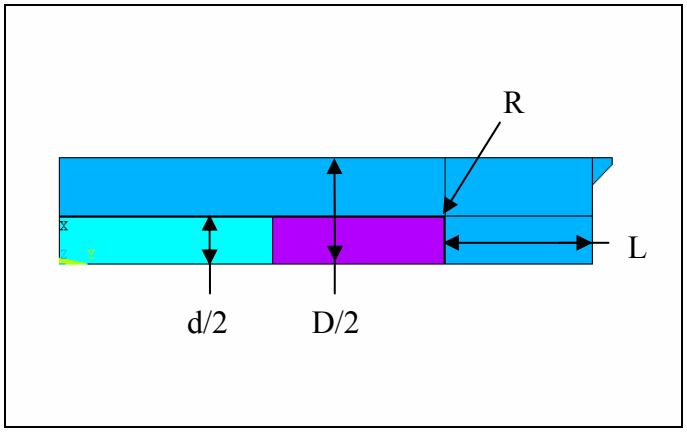

Figure 8 – Components layout for concept 1

In reference to table 1 and figure 8, the tungsten projectile diameter (d) is 22 mm and the sabot diameter (D) is 49.8 mm. These diameters dimension will stay the same for all other concepts. The length of sabot in the rear part of the projectile (L) is 36 mm.

The radius of the projectile edge (R) is equal to 0 mm by the presence of a sharp edge.

Simulation results

Figure 9 shows the sabot simulation result for the stress in the xy-axis. A stress concentration occurred at the projectile edge (See the black circle). The maximum stress was around 82.8 MPa at this edge. The admissible value for the polycarbonate is 63.4 MPa. This means that a failure in shear will occur firstly at this edge for a concept with polycarbonate material.

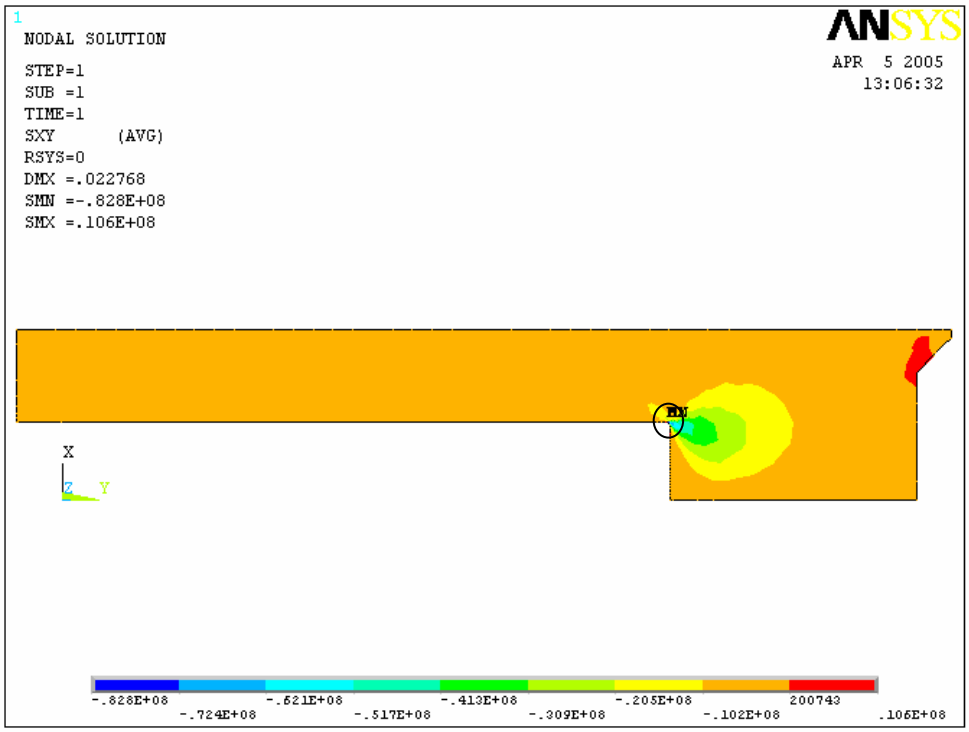

Figure 9 – Sabot stress in xy-axis for concept 1

Figure 10 shows the sabot simulation result for the stress in the y-axis. The maximum stress occurred behind the projectile at the rear part of the sabot. The maximum stress was around 151 MPa at this place. The admissible value of compression for the polycarbonate is 79.3 MPa. This last value represents the stress of compression when a deformation equivalent to 10 % occurred. This means the rear part of the sabot particularly will have a deformation higher than 10 % in compression. It is also important to mention that the stress in compression in the rear part of the sabot showed a higher stress than the sidewall. Also, a maximum tensile stress occurred close to the edge of the sabot. This maximum value was around 158 MPa. This value was over the admissible value of 72.4 MPa for the tensile strength of polycarbonate. This means a failure in compression/tension will occur firstly at this edge for a concept with polycarbonate material.

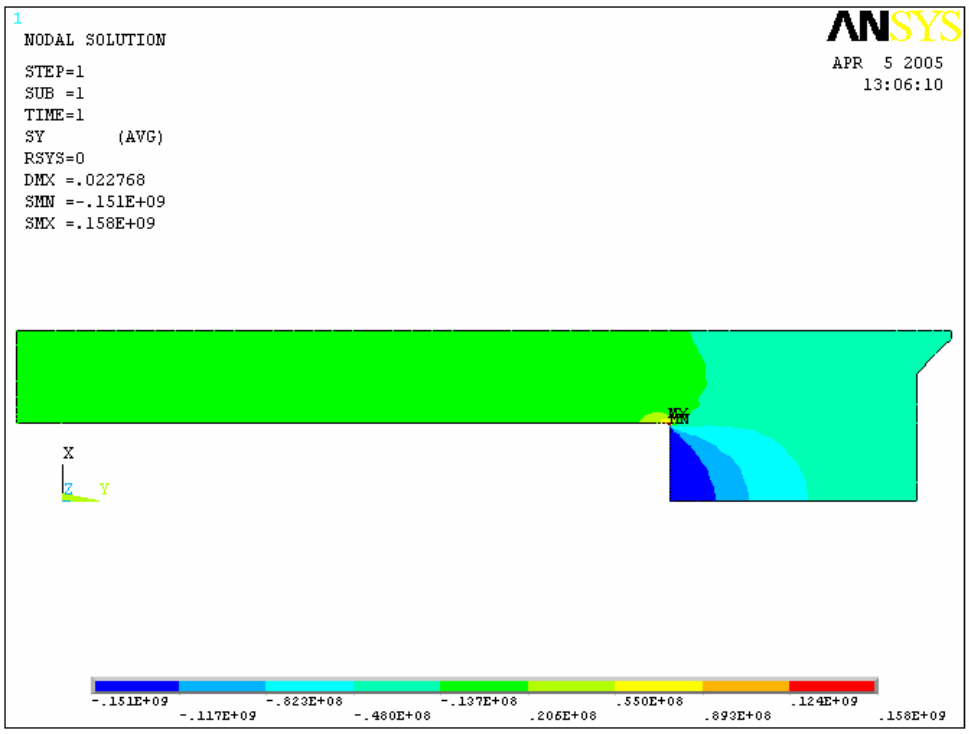

Figure 10 – Sabot stress in y-axis for concept 1

Conclusion

The polycarbonate sabot did not resist to the loading at the point of contact with the projectile edge. To improve the design, the next iteration will replace the actual edge between the spacer and the projectile by a transition radius between these components.

3.2.2 CONCEPT 2 – EXTERNAL SHELL WITH A RADIUS

Physical description and dimension details

This concept introduces a modified polycarbonate sabot for the section in contact with the rear part of the polycarbonate spacer. This concept adds a radius on the rear part of the sabot. The radius would reduce the effect of stress concentration at projectile edge. Figure 11 shows the layout of concept 2 assembly. Again, the cyan, purple and blue colours represent respectively the tungsten projectile, the polycarbonate spacer and the polycarbonate external shell.

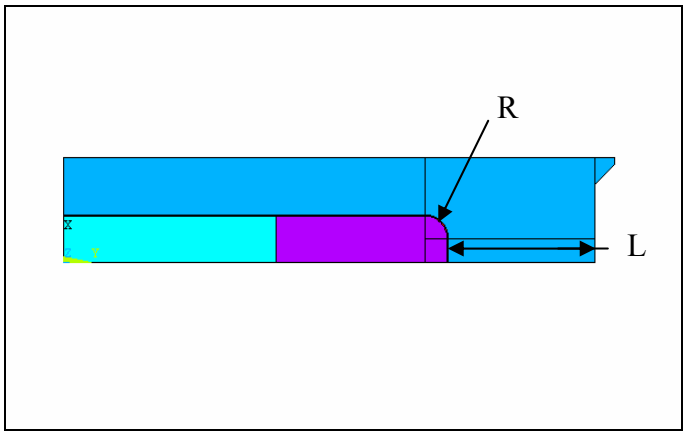

Figure 11 - Components layout for concept 2

The overall sabot and projectile dimensions are the same than for the previous concept. The length of the pusher plate (L) is 36 mm. The calculation SABOT-EC-A-01 is available in appendix B for the calculation detail of the pusher plate length. The radius of the projectile edge (R) is equal to 5.5 mm.

Simulation results

Figure 12 shows the sabot simulation result for the shear stress in the xy-axis. A stress concentration occurred at the radius edge of the projectile (See the black circle).

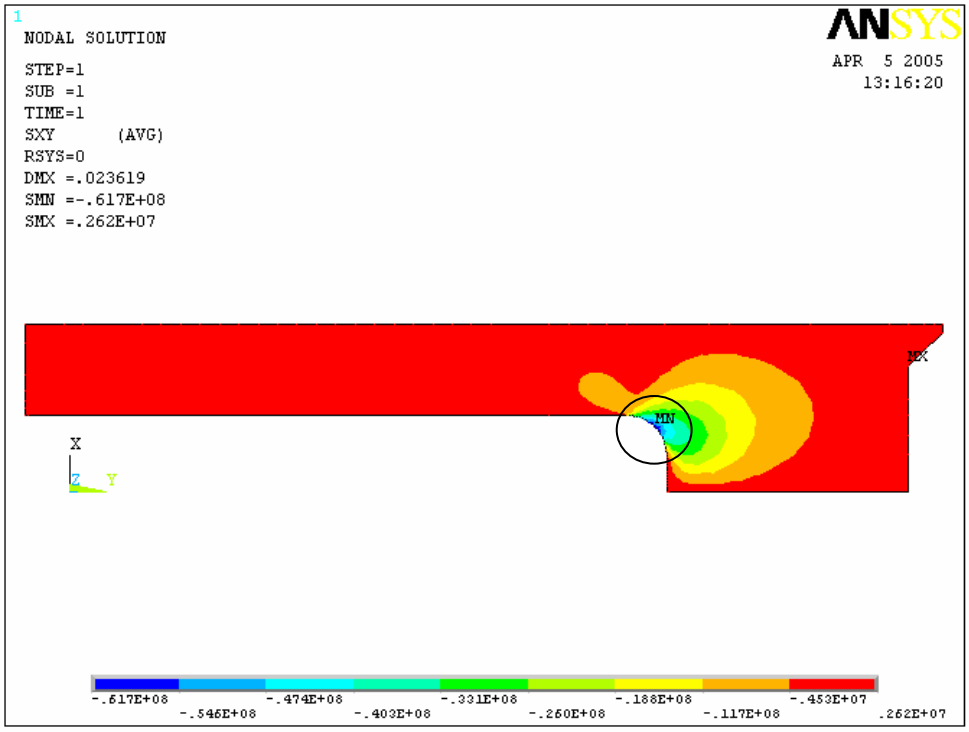

Figure 12 – Sabot stress in xy-axis for concept 2

The maximum stress was around 61.7 MPa at this radius. The admissible value for the polycarbonate is 63.4 MPa. This means the polycarbonate sabot with the radius would resist in shear to the launch in the monolithic design. In comparison with the concept 1, the maximum shear stress has decreased by 25 %.

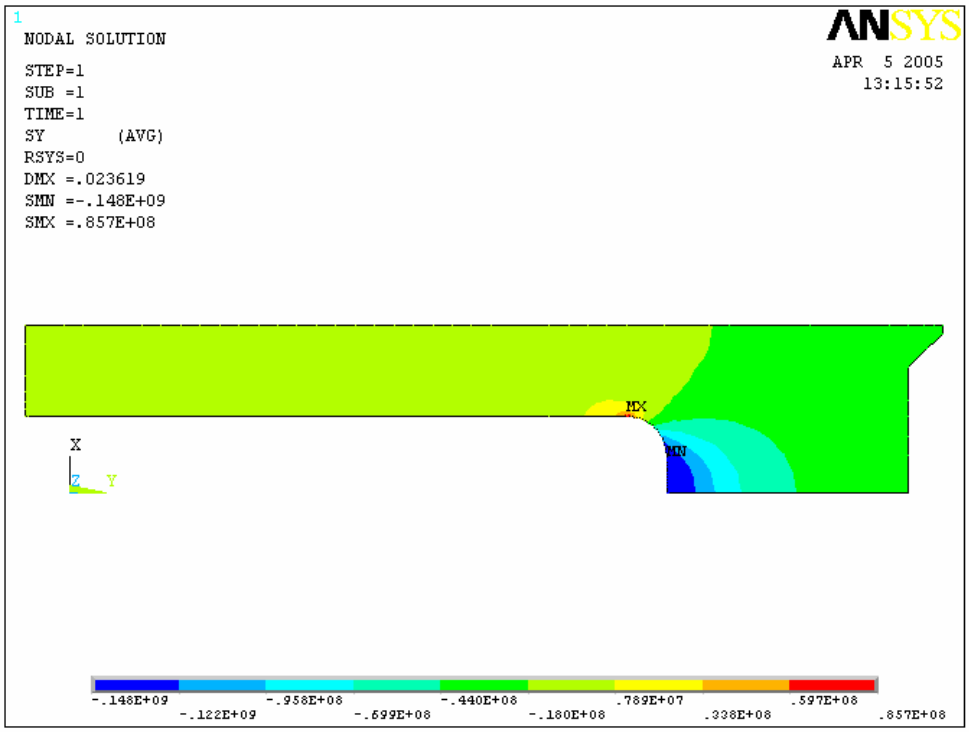

Figure 13 – Sabot stress in y-axis for concept 2

Figure 13 shows the sabot simulation result for the stress in the y-axis. The maximum stress occurred behind the projectile at the rear part of the sabot. The maximum stress was around 148 MPa at this place. The admissible value of compression for the polycarbonate is lower with 79.3 MPa. As for the preceding concept, the stress in the rear part of the sabot showed a higher stress compared to the sidewall. Also, a maximum tensile stress occurred close to the radius of the sabot. This maximum value was around 85.7 MPa. This value was over the admissible value of 72.4 MPa for the tensile strength of polycarbonate. In comparison with the concept 1, the maximum compression stress has decreased by 2 % and the maximum tensile stress, by the introduction of a radius, has decreased by 45 %. This means a failure in compression/tension will occur firstly at this edge for a concept with polycarbonate material.

Conclusion

Because the polycarbonate sabot did not resist on some aspect of the loading at the contact with the spacer of the projectile, it would be interesting to change the material in this area by a stronger material.

3.2.3 CONCEPT 3 – PUSHER PLATE WITH A RADIUS

Physical description and dimension details

This concept introduces an Ultem pusher plate in the rear part of the projectile. This concept adds a pusher plate in the rear part of the sabot. and increases the pusher plate diameter. The radius should reduce the effect of stress concentration at projectile edge. As for the previous concept, the projectile and the pusher plate were loaded by the rear of the sabot. Figure 13 shows the layout of concept 3 assembly. Again, the cyan, purple and red colours represent respectively the tungsten projectile, the polycarbonate external shell and the Ultem pusher plate.

This concept introduces a stronger material part behind the projectile. The stronger material is introduced in the sabot assembly by a pusher plate component. A pusher plate is generally used as a stronger transition material to resist the higher load at the projectile and distribute it on the softer material of the sabot. In this concept, the pusher plate uses the Ultem as material. Figure 14 shows the layout of the concept 3 assembly. The cyan, purple, blue and pink colours represent respectively the tungsten projectile, the polycarbonate the Ultem pusher plate and the polycarbonate external shell. The latter is defined as the external part in diameter of the launch package, i.e. the component in contact with the canon interior bore. From now, the term sabot will describe all components except the tungsten in the launch package. Also, the next figure shows that the pusher plate and the projectile are loaded in the external shell by the rear.

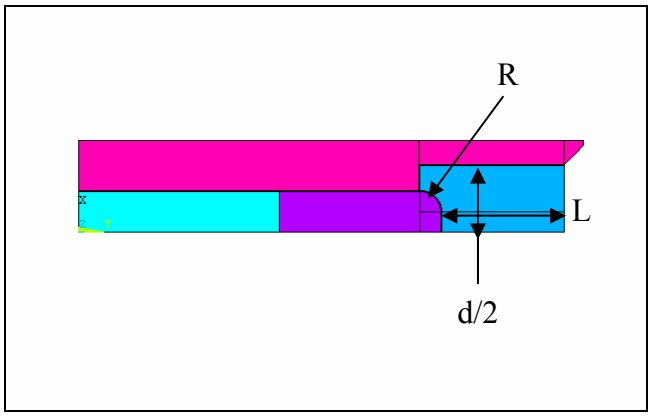

Figure 14 - Components layout for concept 3

The overall sabot and projectile dimensions are the same than for concepts 1 and 2. The length of the pusher plate (L) is 32 mm and the diameter of pusher plate (d) is 36 mm. The preliminary length of the pusher plate came from an old engineering rule, which stipulated that a length of pusher plate is supposed to be equal to his diameter. The distance between the rear of the projectile and the rear of the pusher plate was equal to 32 mm because the pusher plate diameter was 36 mm and a ¾ of radius was considered in the length calculation. The engineering rule included a safety factor

and the analytical calculations gave also a safe value for a length of 32 mm. An optimization of pusher plate length remained possible, but it was not the purpose of the analysis at that time. The calculations SABOT-EC-A-02 and SABOT-EC-A-03 are available in appendix B for the calculation detail of the pusher plate and the sabot length. The radius of the projectile edge (R) is equal to 5.5 mm.

Simulation results

Figure 15 shows the pusher plate simulation result for the stress in the xy-axis. A stress concentration occurred at the projectile radius. The maximum stress was around 54.1 MPa at this place. The admissible value for the Ultem is 103.4 MPa. This means the pusher plate with the radius would resist in shear to the launch in a sabot with a rear loading capability for the monolithic design.

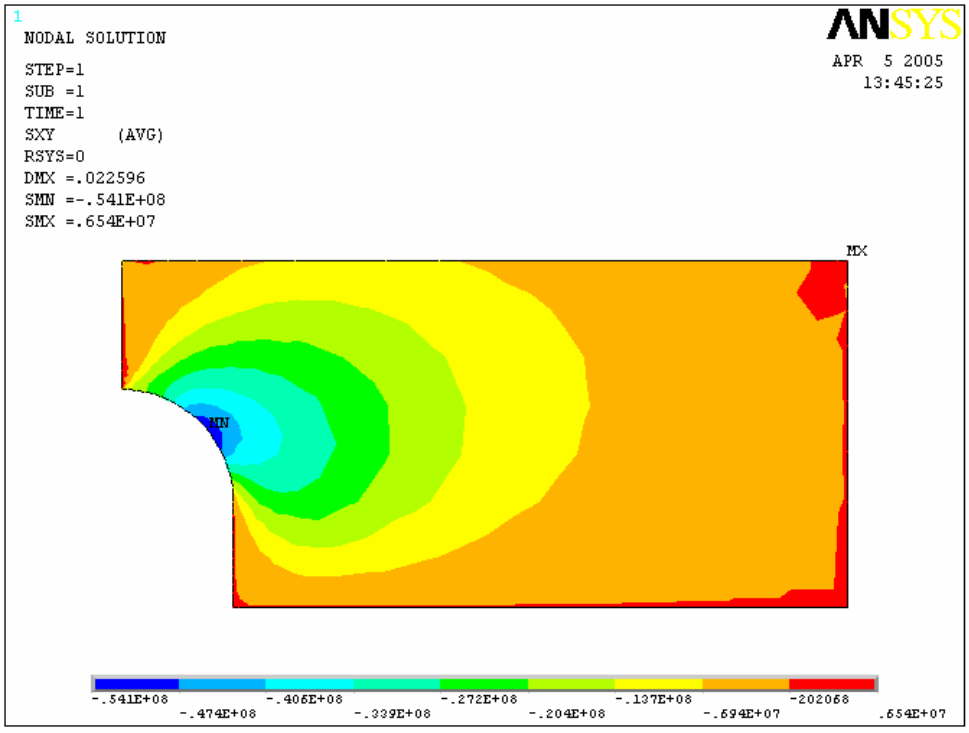

Figure 15 – Pusher plate stress in xy-axis for concept 3

Figure 16 shows the pusher plate simulation result for the stress in the y-axis. On that part, a maximum stress occurred rear the spacer of the projectile. This maximum value was around 148 MPa. This value was under the admissible value of 151.7 MPa for the Ultem. The tensile stress in this concept was not quite important with a small value of 7.28 MPa in comparison with the admissible value of 113.4. This means the pusher plate with the radius would resist in compression to the launch in a sabot with a rear loading capability for the monolithic design.

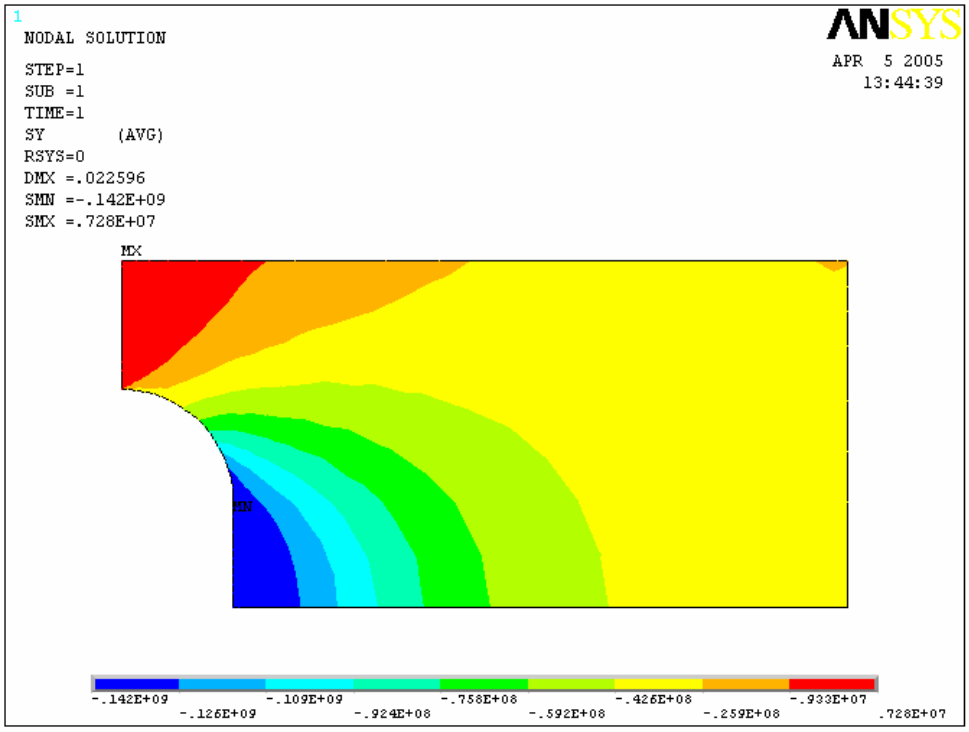

Figure 16 – Pusher plate stress in y-axis for concept 3

Figure 17 shows the consequence the spacer compression would have on the radial stress of the sabot (x-axis).

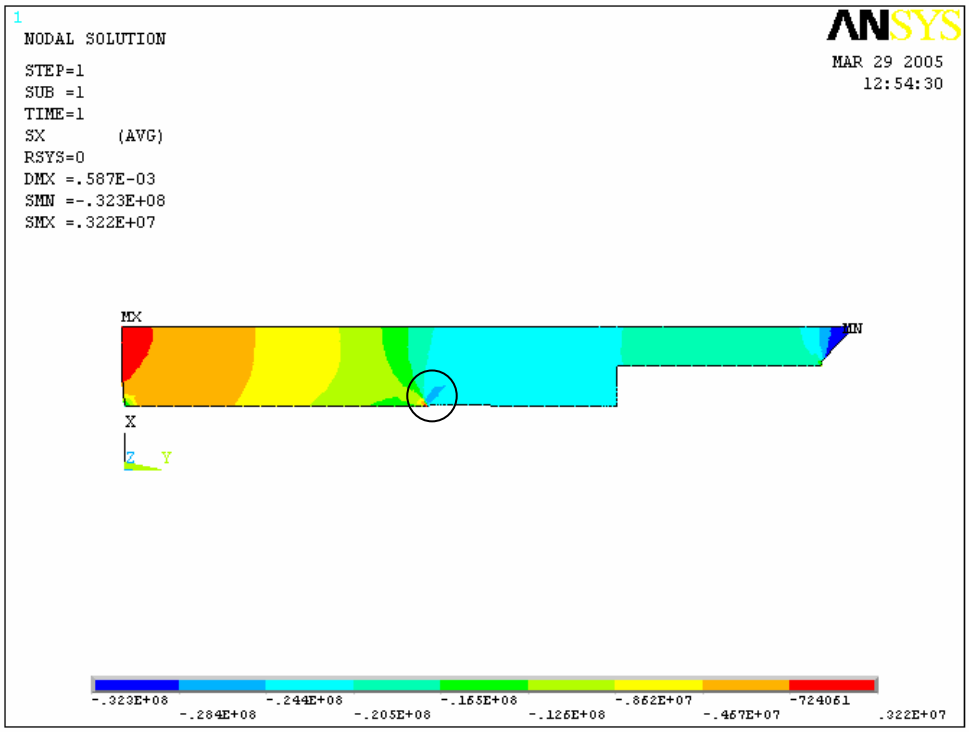

Figure 17 – Sabot stress in x-axis for concept 3

The simulation was done with the assumption that the sabot was still in the canon and a backpressure of 200 MPa was applied to it. The maximum stress occurred at the joint between the tungsten projectile and the polycarbonate spacer (See the black circle). This maximum value was around 28.4 MPa. This value was under the admissible value of 72.4 MPa for the polycarbonate. This means the sabot would resist in the radial stress to the launch of a sabot with a rear loading capability for the monolithic design.

Figure 18 shows the consequence the spacer compression could have on the circumferential stress of the sabot (z-axis). While the sabot is in the launch tube, the confinement prevent expansion of the sabot. This prevents tensile stress to apply in the sabot component walls. It was assumed that when the sabot exits the launch tube is then a worst case condition with regard with z-axis stress. The simulation was done with the assumption that the sabot was out of the canon and a pressure of 165 MPa back pressure was still applied to it. This pressure was equivalent to the point 19 of figure 5. As for the previous figure, the maximum stress occurred at the joint between the tungsten projectile and the polycarbonate spacer (See the black circle). This maximum value was around 31 MPa. This value was under the admissible tensile value of 72.4 MPa for the polycarbonate. This means the sabot would resist the circumference stress to the launch of a sabot with a rear loading capability for the monolithic design.

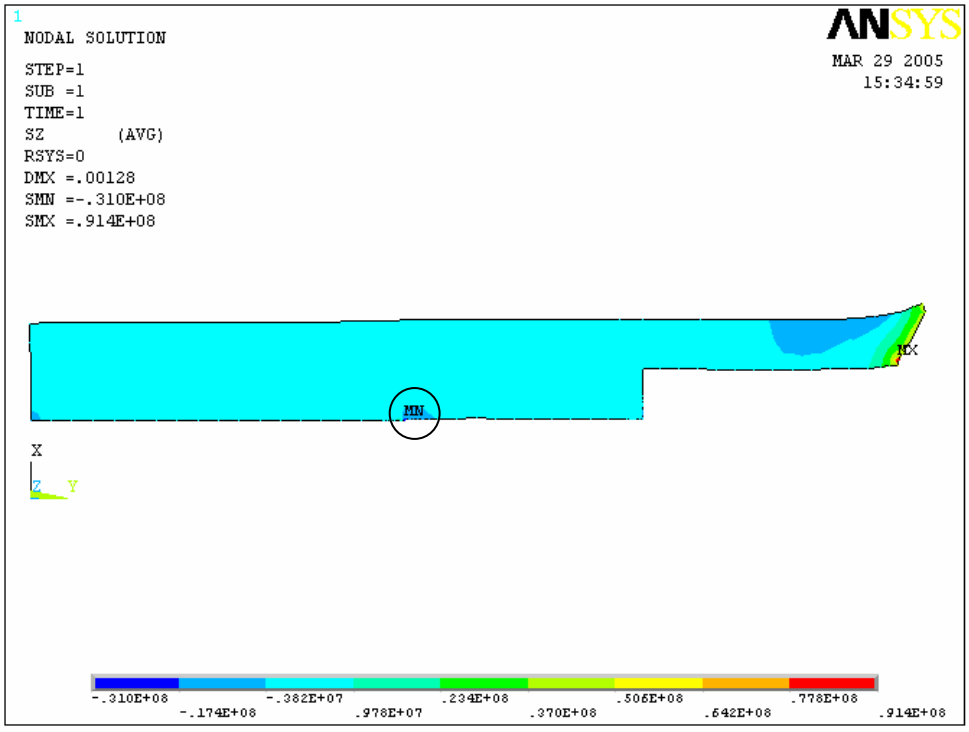

Figure 18 – Sabot stress in z-axis for concept 3

Conclusion

The pusher plate with a radius and the designed sabot would resist the loading for a monolithic design. This design had to be validated for a segmented projectile.

3.2.4 CONCEPT 4 – PUSHER PLATE ON SEGMENTED CONCEPT

Physical description and dimension details

This concept introduces the segmented rod design equivalent to the monolithic design in term of tungsten weight and total launch package weight. All carrier components have the same characteristics and dimensions as for the previous concept. Figure 19 shows the layout of concept 4 assembly.

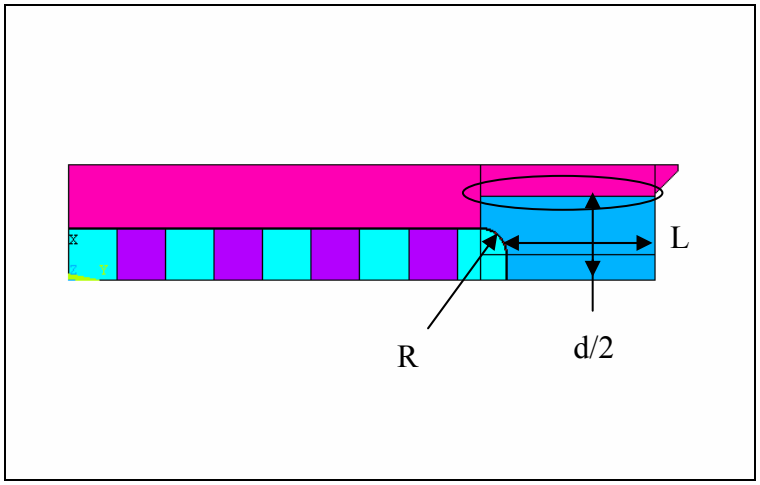

Figure 19 - Components layout for concept 4

The cyan and purple colours represent respectively the tungsten segment and the polycarbonate spacers as components of the projectile. In this concept, 5 tungsten segments and 4 spacers occupy the projectile volume. The blue and the pink represent respectively the pusher plate and the external shell. The pusher plate is in Ultem while the external shell is in polycarbonate. The definitions and dimensions of R, L and d are the same as before.

Simulation results

Figure 20 shows the pusher plate simulation result for the stress in the xy-axis. A stress concentration occurred at the projectile radius. The maximum stress was around 54 MPa at this place. The admissible value for the Ultem is 103.4 MPa. In comparison with the similar monolithic design simulation, the shear value is almost the same. This means the pusher plate with the radius would resist in shear to the launch of a sabot with a rear loading capability for the segmented design.

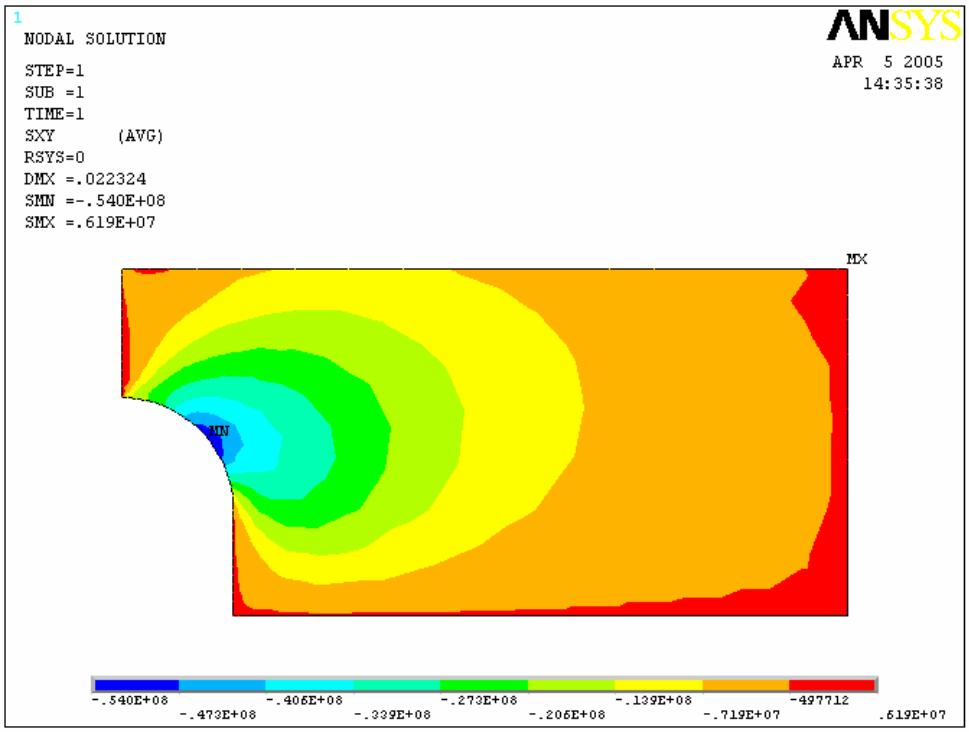

Figure 20 – Pusher plate stress in xy-axis for concept 4

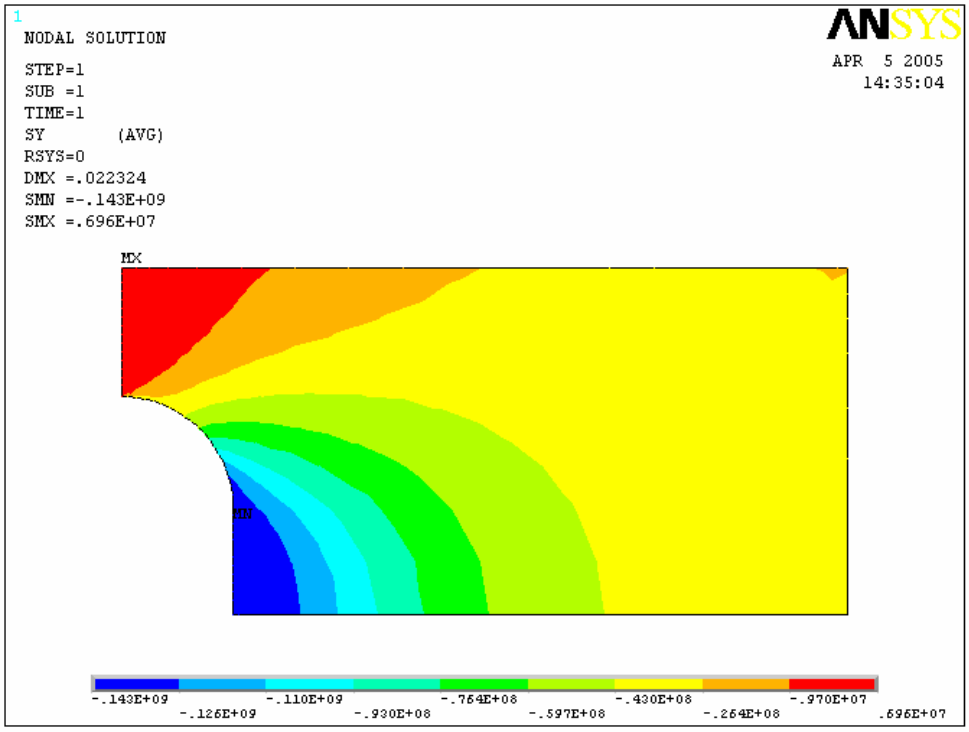

Figure 21 – Pusher plate stress in y-axis for concept 4

Figure 21 shows the pusher plate simulation result for the stress in the y-axis. On this part, a maximum stress occurred rear the spacer of the projectile. As for the previous concept, this maximum value was around 143 MPa. This value was under the admissible value of 151.7 MPa for the Ultem. In comparison with the similar monolithic design simulation, the compression value is almost the same. The tensile stress in this concept was not quite important with a small value of 6.96 MPa in comparison with the admissible value of 113.4. This means the pusher plate with the radius would resist in compression to the launch of a sabot with a rear loading capability for the segmented design.

Figure 22 shows the consequence the spacers compression could have on the radial stress of the sabot. The simulation was done with the assumption that the sabot was still in the canon and a pressure of 200 MPa was applied to it. The maximum stress occurred on the sabot at each position of polycarbonate spacer (Black arrows show the polycarbonate spacer position in the design. The stress value was almost the same for each spacer with a maximum around 32.5 MPa. This value was under the admissible value of 72.4 MPa for the polycarbonate. This means the sabot would resist the radial stress to the launch of a sabot with a rear loading capability for the segmented design. In comparison with the similar monolithic design simulation, the radial stress value was higher by 14 %.

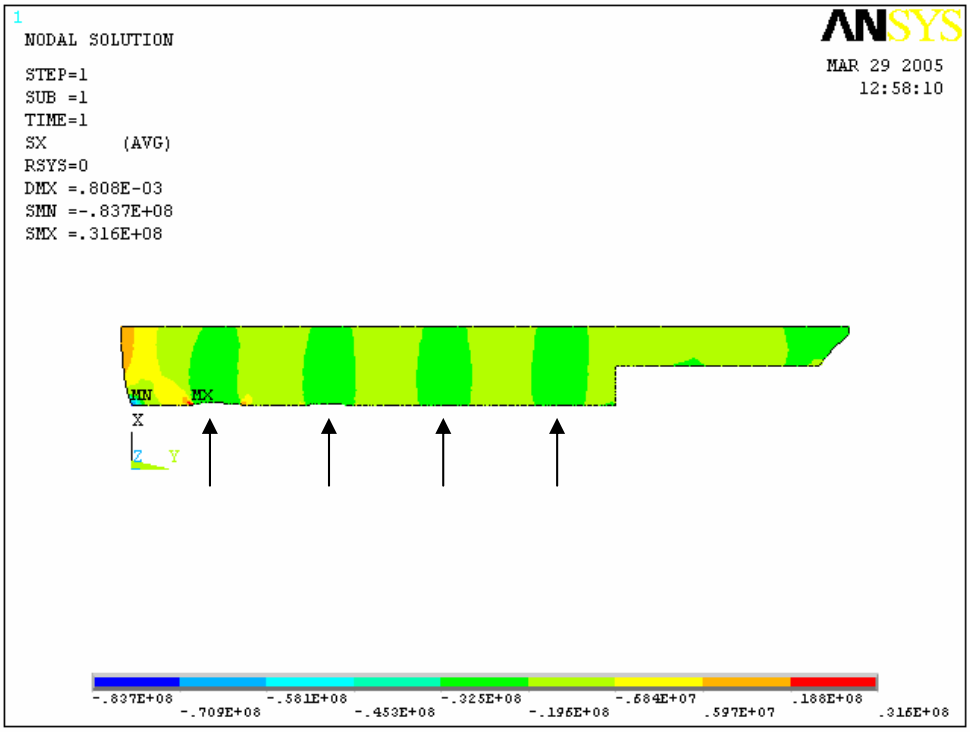

Figure 22 – Sabot stress in x-axis for concept 4

Figure 23 shows the consequence the spacers compression could have on the circumferential stress of the sabot. The simulation was done with the assumption that the sabot was out of the canon and a pressure of 165 MPa was applied to it. This pressure is equivalent to the point 19 of figure 5. As for the previous figure, the maximum stress occurred on the sabot at each position of polycarbonate spacer (Black arrows show the polycarbonate spacer position in the design). The stress value was almost the same for each spacer except for the first one where the value was higher with 36.1 MPa (See the black circle). This value was under the admissible tensile value of 72.4 MPa for the polycarbonate. This means the sabot would resist the radial stress to the launch of a sabot with a rear loading capability for the segmented design. In comparison with the similar monolithic design simulation, the circumference stress value was higher by 16 %.

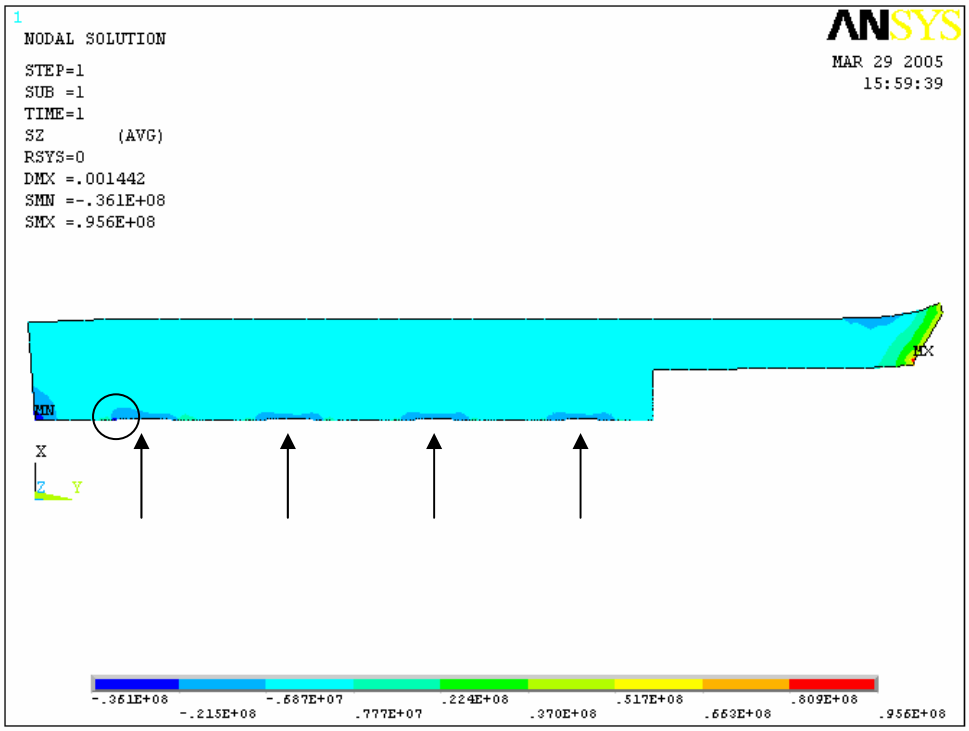

Figure 23 – Sabot stress in z-axis for concept 4

The simulations results of figures 17, 18, 22 and 23 showed that the lateral compression effect on sabot were more important with the segmented design than with the monolithic one.

Analytic calculation results

In this concept, all components are loaded in the external shell by the rear. Some reference with equation 3.2 permitted to realise that the acceleration of the external shell was more important than the acceleration of the components in link with the projectile. A separation would occurred between the external shell and the projectile

during the first time of launch if the shear resistance between the external shell and the pusher plate was not strong enough to restrain the components together (See oval shape on figure 19). This shear resistance must compensate the effect of the acceleration difference for the components. Equation 3.3 presents the relation between the acceleration effect and the shear resistance. The two lines, which following in equation, plugged values in link with the concept 4 to evaluate how far the assembly would function if it was loaded by the rear.

$$(a_{Externalshell} - a_{\Pr ojectile}) \cdot M_{ExternalShell} \leq \mathrm{S}_{\mathrm{shear}} * \mathrm{A}_{\mathrm{shear}} * \mathrm{M}_{\mathrm{f}\ \langle Externalshell / \Pr ojectile \rangle} \quad (3.3)$$

$$((870790) - (407150)) \times 0.210) \leq (63.4 \cdot 4241 \cdot 0.35)$$

$$97364 \leq 94107$$

Where $a_{\text{external shell}}$ is the acceleration of the sabot
$a_{\text{projectile}}$ is the acceleration of the components in link with the projectile
$M_{\text{external shell}}$ is the mass of the external shell
S_{shear} is the shear strength of material
A_{shear} is the shear area of the surface between the external shell and the projectile
M_f is the factor associated with the type of mechanical restraint systems.

If equation 3.3 was true, the external shell and the projectile would remain together, because the shear force would be at least equal to the difference effect of the acceleration. The calculation SABOT-EC-A-04 is available in appendix B for the calculation detail of the necessary thread length for a rear loading sabot.

In concept 4, the separation between the components will occur between the external shell and the projectile components even if the shear resistance between the external shell and the pusher plate was considered. In fact, the values of table 3 have been inserted in the equation 3.3, the result showed that the shear stress of the actual thread was not enough to maintain the projectile and the external shell together.

Table 3 – Data acceleration difference

Term of in equation	Value
$a_{\text{external shell (m/s^2)}}$	870 790
$a_{\text{projectile (m/s^2)}}$	407 150
$M_{\text{external shell (kg)}}$	0.210
$S_{\text{shear (MPa)}}$	63.4
$A_{\text{shear (mm^2)}}$ (PI()*D*L)	4241
$M_{f\,\text{(Thread)}}$	0.35

The value of Mf = 0.35 came from a calculation SABOT-EC-E-06 available in appendix B. This calculation showed that a thread had a resistance in shear around 35 % of the material value. This means a pusher plate and a sabot in the same piece with a stronger material should resist to the pressure in a rear loading design.

Conclusion

In reference with the analysis of previous part, the concept of the sabot loaded by the rear was impossible for the components dimension of this concept. This is mainly because the shear resistance between the external shell and the pusher plate was too low in comparison with the effect of acceleration difference. It is impossible to consider, without a good optimization process, a concept loaded by the rear for that kind of small dimensions. In this condition, the next concept will load all the components in the launch package by the front part.

3.2.5 CONCEPT 5 – CONCEPT WITH A FRONT LOADING

Physical description and dimension details

This concept introduces the loading of all the components inside the external shell by the front. By this fact, the shape of external shell has been changed to add material rear the pusher plate. This concept introduces two new components: the internal sleeve and the front cover. The internal sleeve permits to fill the large hole necessary to ensure the loading of the pusher plate by the front. The front cover permits to keep components together inside the external shell. It is distinct of the external shell component, but threaded to it.

Figure 24 shows the layout of concept 5 assembly. The cyan, purple, red and blue colours represent components already presented in previous concept. These colours represent respectively the tungsten projectile, the polycarbonate spacers, the polycarbonate external shell and the Ultem pusher plate. The yellow and the green colour represent the new components introduced in this concept. These two colours represent respectively the Ultem internal sleeve and the polycarbonate cover. The internal sleeve is in Ultem to keep a safety factor 50 % higher in the design for a difference of only 4 grams if we compare with the polycarbonate material. All the components are loaded by the front.

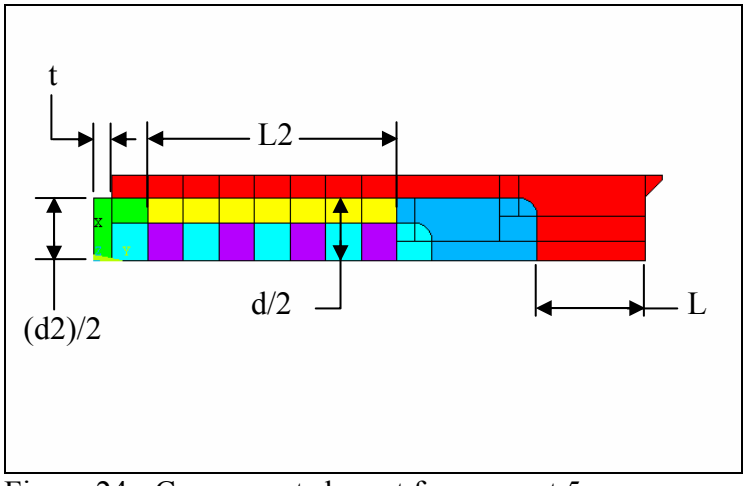

Figure 24 - Components layout for concept 5

In reference to figure 24, the external shell length (L) is 32 mm rear the pusher plate. The external diameter of the internal sleeve (d) is 36 mm and the length (L2) is 73.5 mm. The front cover has a diameter (d2) of 36 mm and a thickness (t) of 5 mm in the front of the projectile. All other dimensions of the components stay the same in comparison with concept 4.

Analysis results

Figure 25 shows the pusher plate simulation result for the stress in the xy-axis. A stress concentration occurred at the radius in contact with the projectile. The maximum shear stress was around 57.5 MPa at this place. The admissible value for the Ultem is 103.4 MPa. This means the pusher plate with the radius would resist in shear to the launch of the front-loading segmented design. In comparison with the rear loading segmented design, the shear stress value is higher by 6 %.

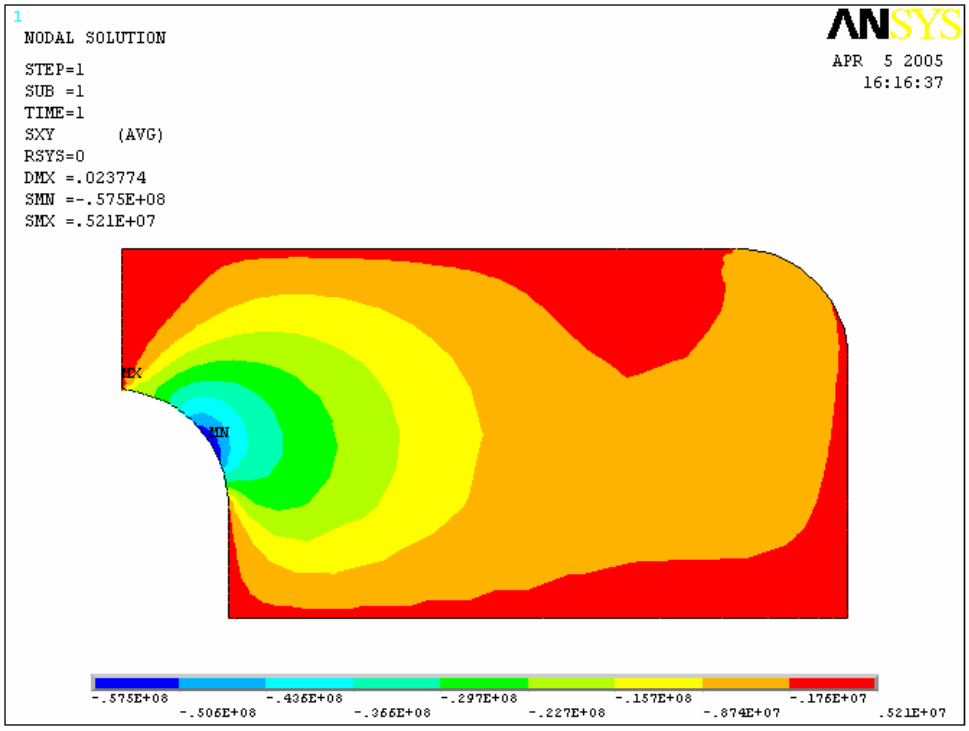

Figure 25 – Pusher plate stress in xy-axis for concept 5

Figure 26 shows the external shell simulation result for the stress in the xy-axis. A stress concentration occurred at the radius in contact with the pusher plate. The maximum shear stress was around 20.4 MPa at this place. The admissible value for the polycarbonate is 72.4 MPa. This means the external shell with the radius would resist in shear to the launch of the front-loading segmented design.

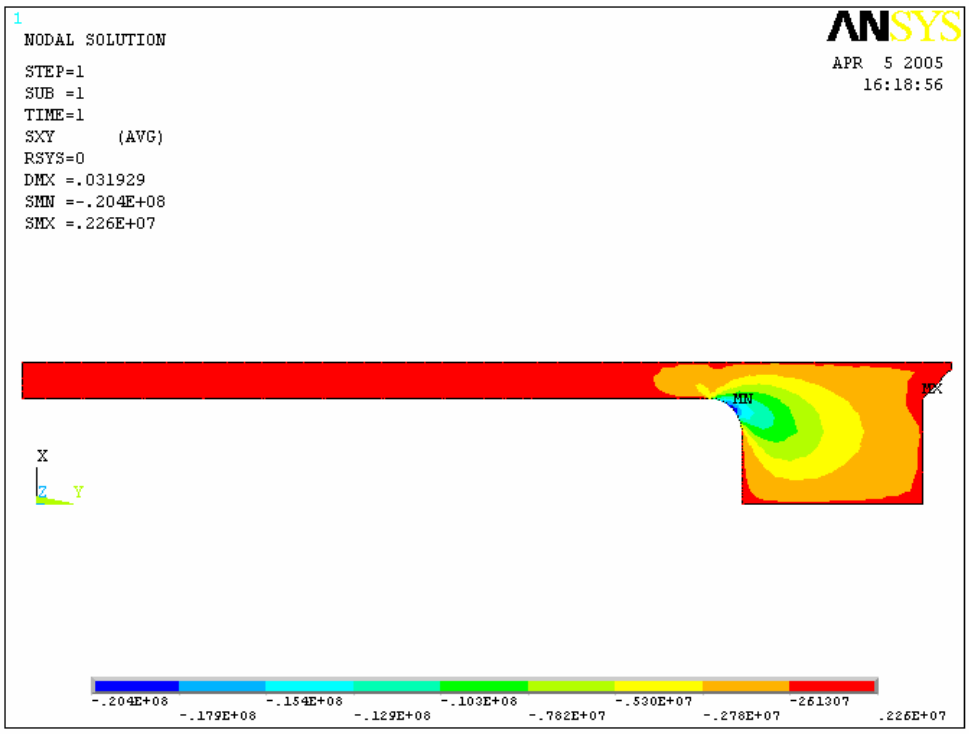

Figure 26 – External shell stress in xy-axis for concept 5

Figure 27 shows the pusher plate simulation result for the stress in the y-axis. On this part, a maximum compression stress occurred rear the last segment of the projectile. This maximum value was around 151 MPa. This value was under, but very close to the admissible value of 151.7 MPa for the Ultem. This means the pusher plate with the radius was border line in term of resistance in compression to the launch of the front-loading segmented design. In comparison with the rear loading segmented design, the compression stress value was higher by 6 %.

Figures 26 and 27 had a higher value of shear and compression by a factor around 6 % compare to the concept with a loading by the rear. This could be explained by the fact that all the pressure must pass by the pusher plate in this kind of configuration.

Figure 28 shows the external shell simulation result for the stress in the y-axis. On this part, a maximum compression stress occurred rear the pusher plate. This maximum value was around 56.4 MPa. This value was under the admissible value of 79.9 MPa for the compressive strength of polycarbonate. Also, a maximum tensile stress of 24.3 Mpa occurred at the end of the radius in link with the sidewall part of the external shell. This value was under the admissible value of 72.4 MPa for the tensile strength of polycarbonate. This means the external shell would resist in tension and compression to the launch in the front-loading segmented design.

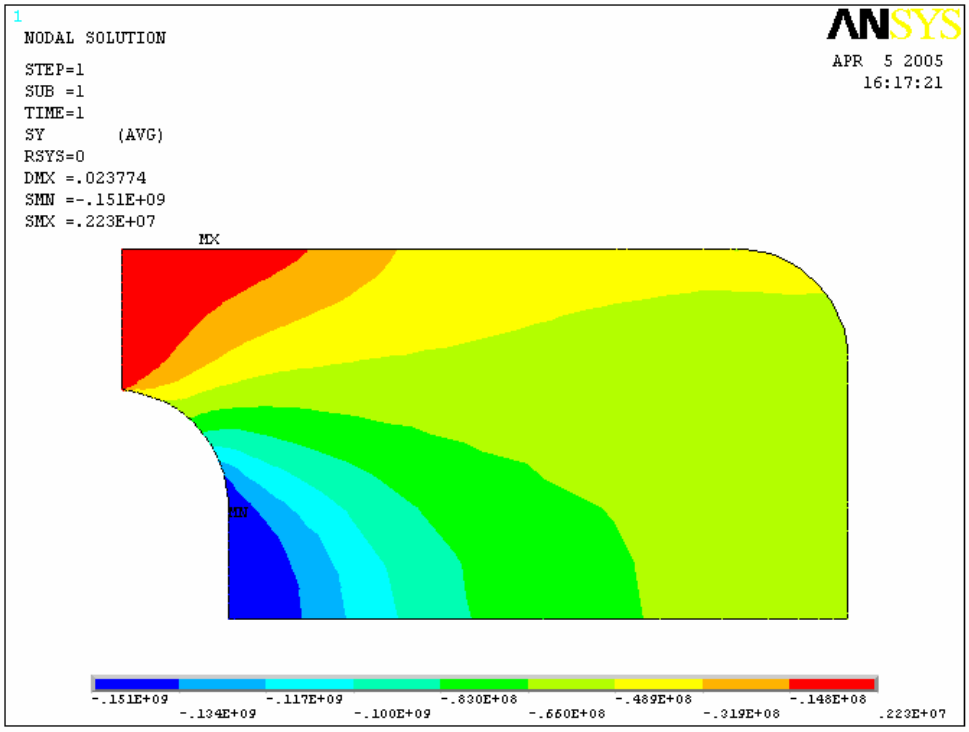

Figure 27 – Pusher plate stress in y-axis for concept 5

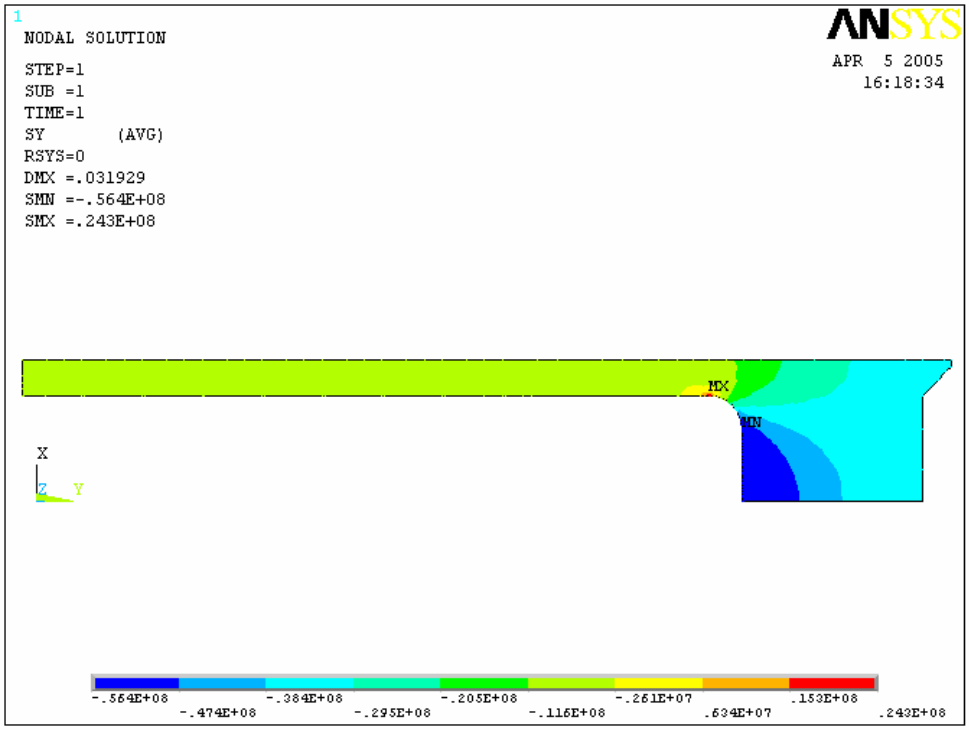

Figure 28 – External shell stress in y-axis for concept 5

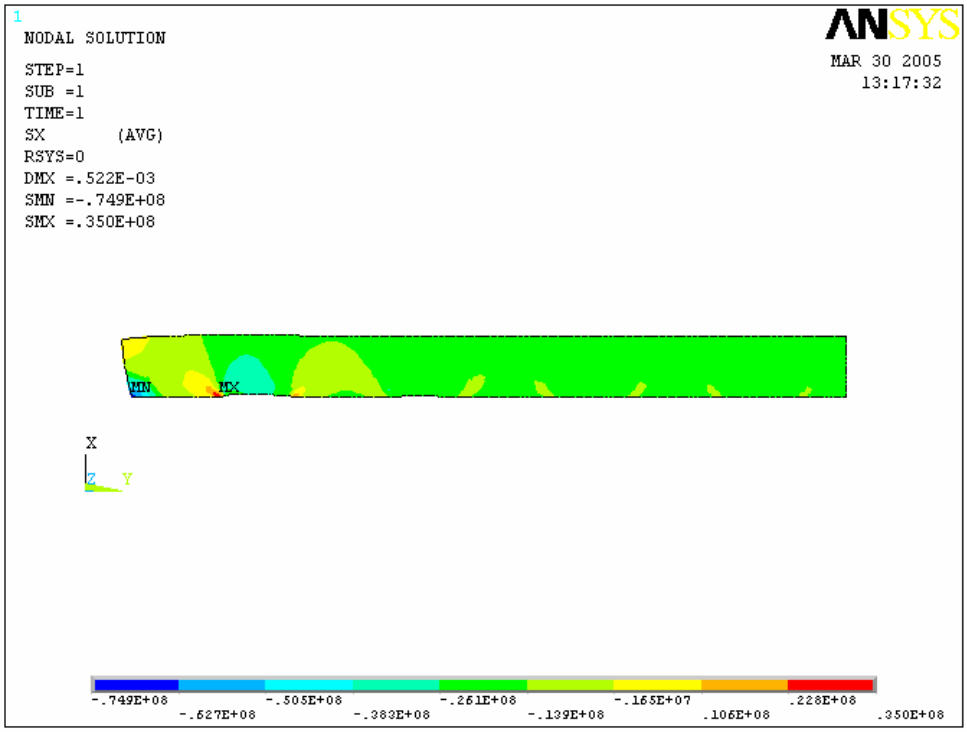

Figure 29 – Internal sleeve stress in x-axis for concept 5

Figure 29 shows the consequence the spacers compression could have on the radial stress of the internal sleeve. The simulation was done with the assumption that the sabot was still in the canon and a pressure of 200 MPa was applied to it. The maximum stress occurred on the internal sleeve at the first polycarbonate spacer position (See the black circle). The maximum stress value caused by the first polycarbonate spacer was around 38.8 MPa. This value was under the admissible value of 113.4 MPa for the Ultem. This means the internal sleeve would resist in the radial stress for the launch of a sabot with a front loading capability for the segmented design. In comparison with the rear loading design simulation, the radial stress value is higher by 19 %.

Conclusion

The concept loaded by the front had shown interesting results in term of resistance. It was ready for the fabrication of a first prototype to try a launch. This concept was designed to have the same components such as the external shell, the internal sleeve, the pusher plate and the front cover, either for the monolithic or the segmented projectile.

3.2.6 SUMMARY OF CONCEPT FOR STATIC ANALYSIS

Table 4 gives a summary about the preliminary static analysis concepts. The design types mentioned by a letter correspond to the Monolithic (M) or Segmented (S) as defined in Section 2.1. The sabot components defined by the letters ES and PP are respectively the External Shell and the Pusher Plate. The sabot material uses the letters P or U respectively for the Polycarbonate or for the Ultem and represents the material of the component for the row above.

Table 4 – Summary of the characteristics and results for the static analysis concept

Descriptions	C-1	C-2	C-3	C-4	C-5
Design type	M	M	M	S	S
Sabot components	ES	ES+PP	ES+PP	ES+PP	ES+PP
Sabot material	P	P+U	P+U	P+U	P+U
Radius at projectile end (mm)	0	5.5	5.5	5.5	5.5
Pusher plate diameter (mm)	No PP	No PP	36	36	36
Projectile introduction end	Front	Rear	Rear	Rear	Front
Reference section number	3.2.1	3.2.2	3.2.3	3.2.4	3.2.5

4.0 CONCEPTUAL MODEL ANALYSIS FOR EXPERIMENTATION

4.1 FIRST LAUNCH SABOT CONCEPT ANALYSIS RESULTS

This section gives all detailed results in regard with the first launch concept chosen for the preliminary sabot experimentation in the gas gun. The following sections 4.1.2 and 4.1.3 will cover results in term of analysis types. Particularly, results for analytic and static aspects will be covered.

4.1.1 PRESENTATION OF CONCEPT

This first launch concept is the concept 5, presented in section 3.2.5, but with the monolithic projectile. For the monolithic projectile, the 5 tungsten segments are replaced by one long segment of equivalent mass and the 4 polycarbonate spacers are replaced by one long spacer. The length of the spacer is adjusted so this concept does not bring any changes on the dimensions and material for all the sabot components. Figure 30 shows all the components involved in the launch package of this concept. On this figure, the white parts are in polycarbonate, the brown are in Ultem and the metallic one is in tungsten. Additional pictures of this concept are available in appendix C.

Figure 30 – Components of the first launch concept assembly

Figure 31 shows the layout of the first launch concept assembly. As for the previous concept, the cyan, purple, red, blue, yellow and green colours represent respectively

the tungsten projectile, the polycarbonate spacers, the polycarbonate external shell, the Ultem pusher plate, the Ultem internal sleeve and the polycarbonate cover. All the components are loaded by the front and the cover is screwed on the external shell to close the assembly. Additional detailed drawings of this concept is available in appendix D.

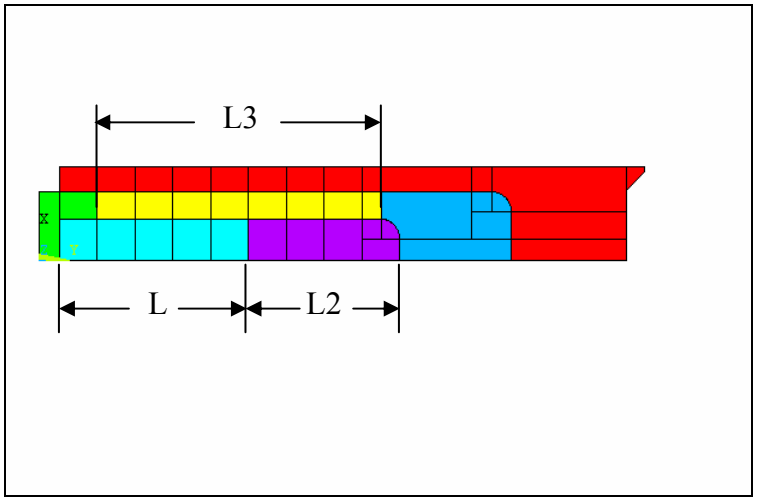

Figure 31 - Components layout for the first launch concept

In reference to figure 31, the projectile segment has a length (L) of 52.5 mm. The spacer behind the projectile has a length (L2) of 42 mm. The internal sleeve has a length (L3) of 79 mm. All other components and dimensions are exactly the same as concept 5.

4.1.2 ANALYTIC CALCULATION RESULTS

This section gives results on the first launch concept in term of shear for components in the rear part of the projectile. These components are the pusher plate and the external shell.

Table 5 gives details about the pusher plate and the external shell dimension in the rear part of the projectile as they are in concept 5. All dimensions are given in mm. As mentioned in the previous section 3.2.3, the calculations SABOT-EC-A-02 and SABOT-EC-A-03 are available in appendix B for the calculation detail of the pusher plate and the external shell length.

Table 5 – Dimensions of components at the projectile rear part for the launch concept 1

Components	Push diameter (mm)	Push length (mm)	Projectile Diameter (mm)
Pusher plate	36	32	22
External shell	49.6	32	36

Table 6 gives details about the maximum stress on the pusher plate and on the external shell to compare with the admissible value. Equation 3.1 has been used to find the maximum stress on the components. An OK value is used when the maximum stress value is lower than the admissible stress.

Table 6 – Analytic stress validation on the rear components for launch concept 1

Components	Maximum stress (MPa)	Admissible stress (MPa)	Validation
Pusher plate	57.6	113.8	OK
External shell	50.5	72.4	OK

Table 6 shows that actual dimensions permit an adequate resistance in the shear aspect for the pusher plate and the external shell of the first launch concept.

4.1.3 STATIC NUMERICAL SIMULATION RESULTS

This section gives the static analysis results on the sabot assembly components such as the pusher plate, the external shell and the internal sleeve around the projectile. The results will be evaluated for the stress in x, xy and y-axis. Figure 32 shows the pusher plate numerical simulation result for the stress in the xy-axis.

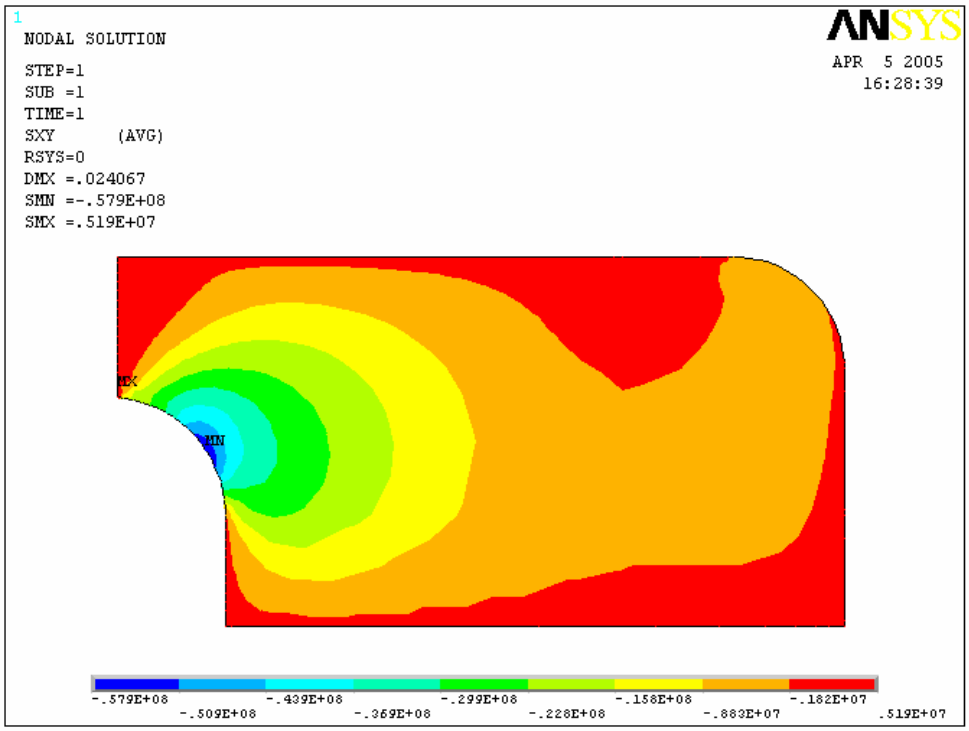

Figure 32 – Pusher plate stress in xy-axis for the launch concept 1

In the previous figure, a stress concentration occurred at the radius in contact with the spacer of the projectile. The maximum shear stress was around 57.9 MPa at this place. The admissible value for the Ultem is 103.4 MPa. This means the pusher plate with these dimensions and this shape would resist in shear to the launch of the front-loading monolithic design.

Figure 33 shows the external shell numerical simulation result for the stress in the xy-axis. A stress concentration occurred at the radius in contact with the pusher plate. The maximum shear stress was around 20.4 MPa at this place. The admissible value for the polycarbonate is 72.4 MPa. This means the external shell with these dimensions and this shape would resist in shear to the launch of the front-loading monolithic design.

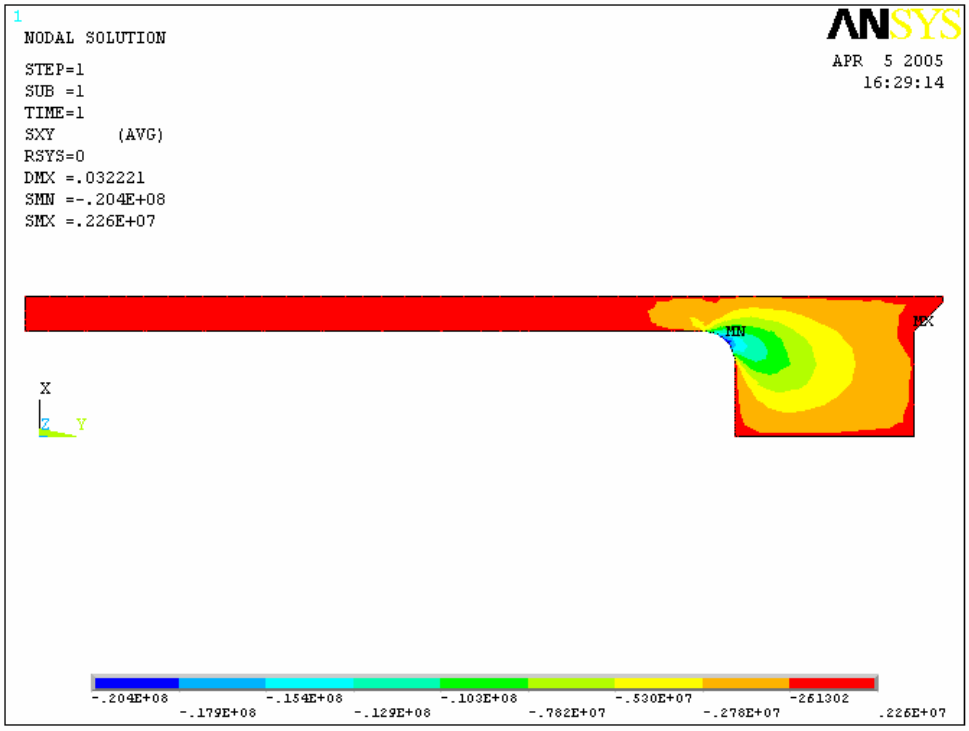

Figure 33 – External shell stress in xy-axis for the launch concept 1

Figure 34 shows the pusher plate numerical simulation result for the stress in the y-axis. On this part, a maximum compression stress occurred rear the spacer of the projectile. The maximum value was around 150 MPa. This value was under, but very close to the admissible value of 151.7 MPa for the Ultem. This means the pusher plate with these dimensions and this shape was border line in term of resistance in compression to the launch of the front-loading monolithic design. Because this admissible stress represent a deformation of 10 % in compression, the limitation is a design factor that permits to the component to do the job under the loading even the maximum stress is very close to the admissible value. In conclusion, the assembly will be launched and will probably success despite this high compression stress value

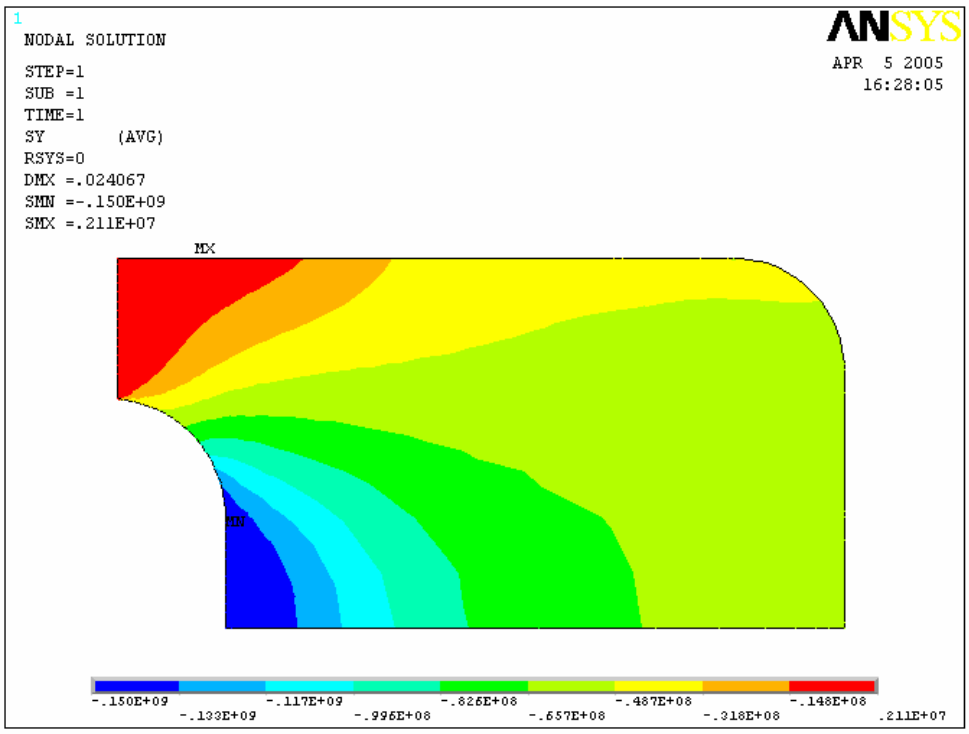

Figure 34 – Pusher plate stress in y-axis for the launch concept 1

Figure 35 shows the external shell numerical simulation result for the stress in the y-axis.

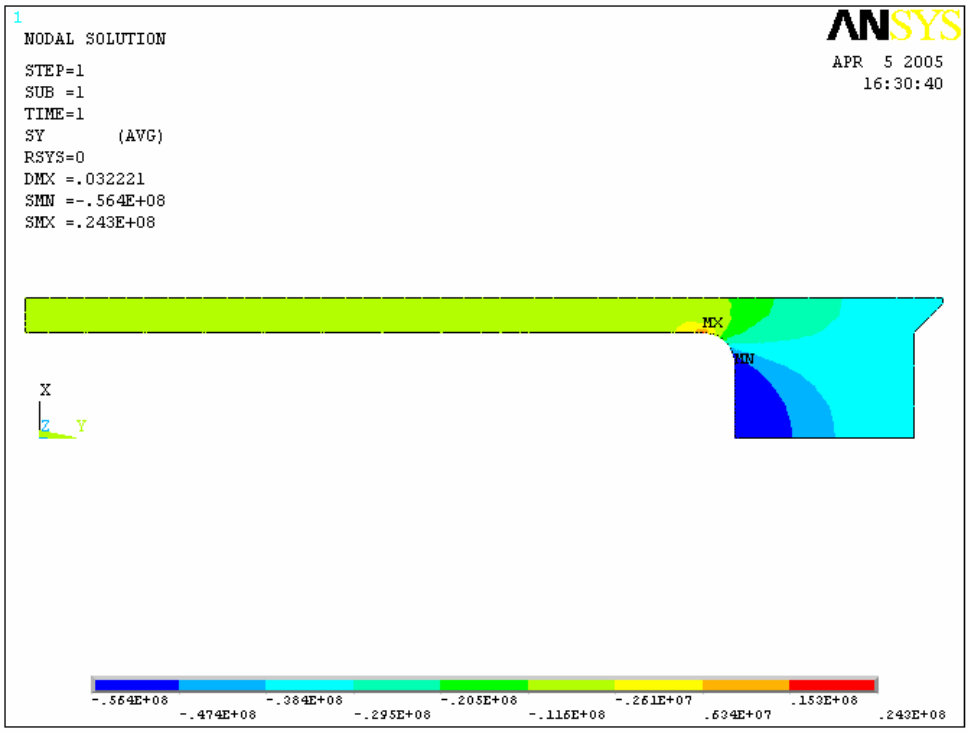

Figure 35 – External shell stress in y-axis for the launch concept 1

In the previous figure, a maximum compression stress occurred rear the pusher plate. This maximum value was around 56.4 MPa. This value was under the admissible value of 79.9 MPa for the compressive strength of polycarbonate. Also, a maximum tensile stress occurred at the end of the radius in link with the sidewall part of the external shell. This maximum value was around 24.3 MPa. This value was under the admissible value of 72.4 MPa for the tensile strength of polycarbonate. This means the external shell would resist in tension and compression to the launch in the front-loading monolithic design.

Figure 36 shows the spacer numerical simulation result for the stress in the y-axis. On this part (See black circle), a stress value of 295 MPa represents the maximum value in compression. This maximum value in compression is over the admissible value of 79.9 MPa for the compressive strength of polycarbonate. Even if the stress in compression is higher than the admissible value it was chosen to keep the spacer in polycarbonate at this point. This was decided firstly because the spacer is confined between the pusher plate, the tungsten projectile and the internal sleeve. At the limit, the spacer will lose its shape, but will keep almost the same volume as before degradation. Secondly, penetration performance optimization requires a spacer fabricated with a lightweight material, as polycarbonate. If a heavier material was used with the tungsten, the expected penetration would decrease. This means, the spacer would not resist to the loading in compression, but the launch would be a success if the spacer stayed confined between other components. This is the weakest point of the first launch concept.

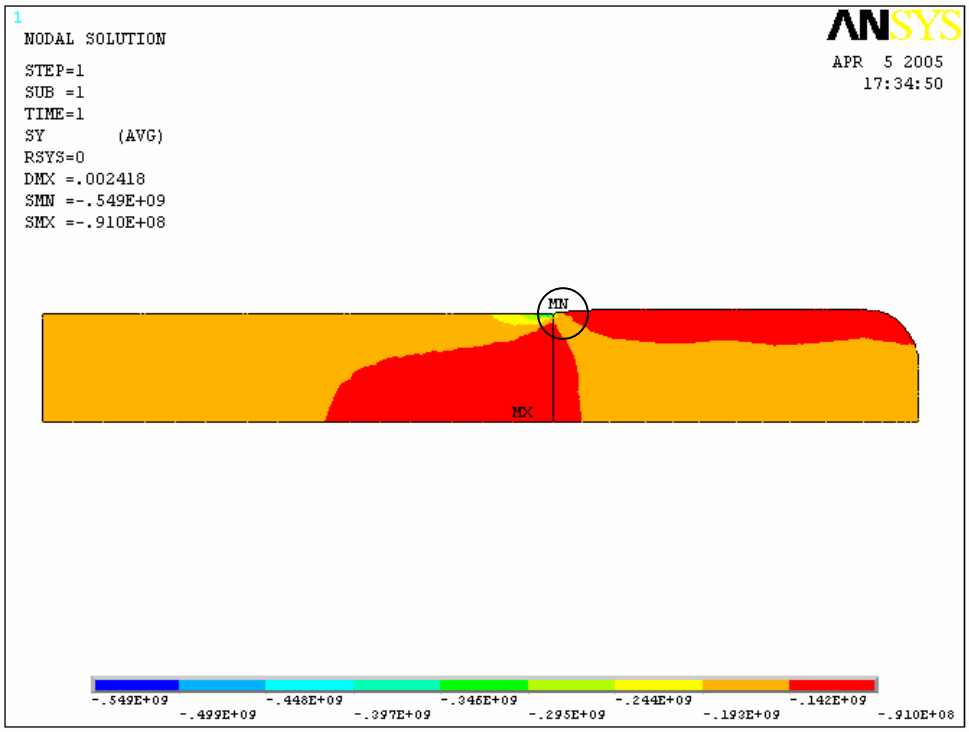

Figure 36 – Segment and spacer stress in y-axis for the launch concept 1

Figure 37 shows the external shell numerical simulation result for the stress in the x-axis. The simulation was done with the assumption that the sabot was still in the canon and a pressure of 200 MPa was applied to it. On the external shell, a maximum radial stress occurred at the joint between the internal sleeve and the pusher plate. This maximum value was around 170 MPa. This value is true if we take the assumption that a relative movement between the internal sleeve and the pusher plate can occur and at the same time increase the pressure on the external shell. This maximum value was over the admissible stress of 72.4 MPa for the tensile strength of polycarbonate. This simulation remained realistic, but represented the worst case.

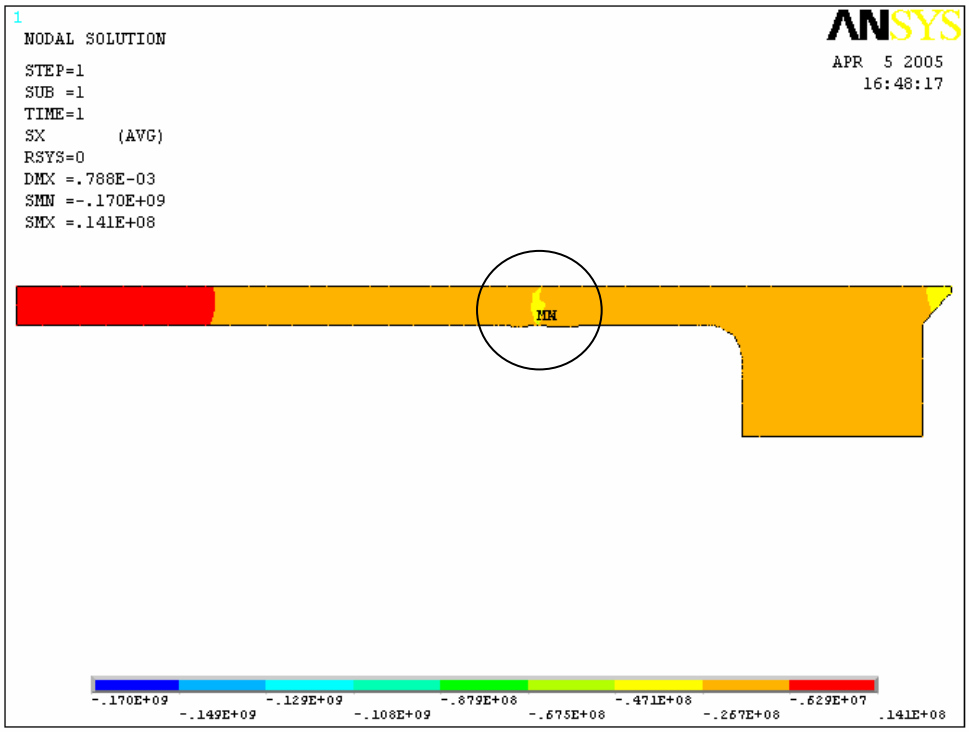

Figure 37 – External shell stress in x-axis for the launch concept 1 according to assumption

At the opposite of the previous case, if there is no gap on the joint between the sleeve and the pusher plate, the simulation of figure 38 presented lower value of stress in x-axis. In fact, the stress value at the joint position was around 20.5 MPa. This value was under the admissible stress of 72.4 MPa for the tensile strength of polycarbonate. This means, the external shell would resist to the radial stress if the joint stayed perfectly between the internal sleeve and the pusher plate. To keep the fabrication aspect simplified, the sleeve and the pusher plate were fabricated in two different components for the launch concept 1.

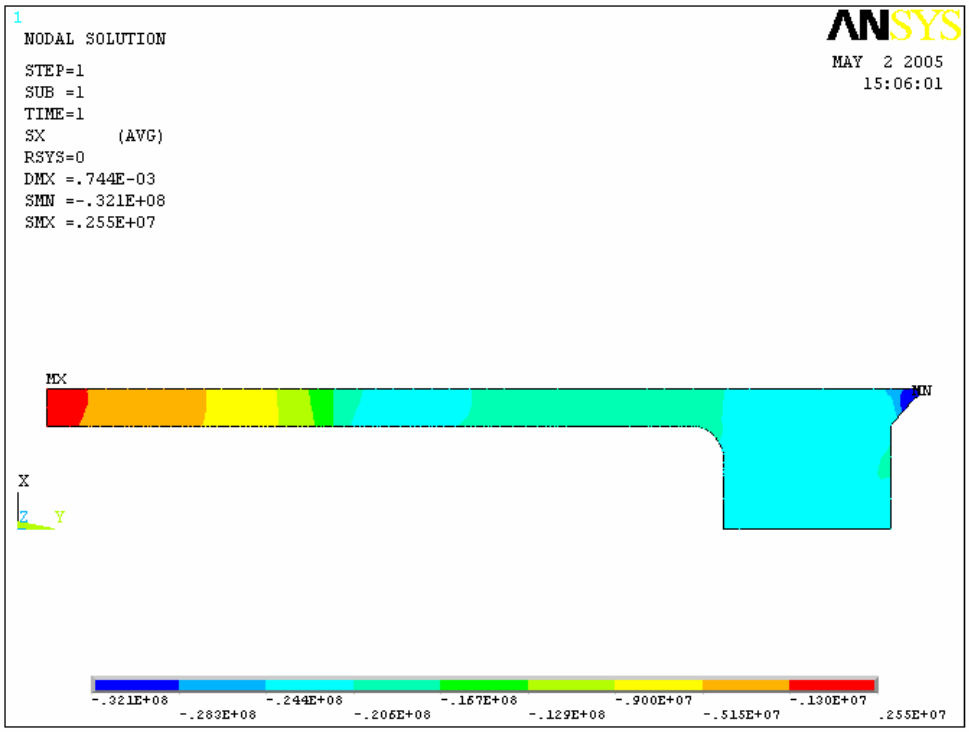

Figure 38 – External shell stress in x-axis for the launch concept 1 according to assumption

4.1.4 LAUNCH RESULTS

This section shows the characteristics of the first launch concept in flight and the damage the sabot suffered before it impacted the target. This concept is linked with experimentation number 17 at the hypervelocity impact laboratory. The total weight of the assembly is 696.5 grams and the total weight of the tungsten is 339.36 grams.

Figure 39 shows an X-ray of the launch package in flight before it reached the target. On this figure, it is possible to see the following points:

- The external shell was broken in flight around the joint between the internal sleeve and the pusher plate (Item 1);
- The polycarbonate spacer was not inside the sleeve (Item 2);
- The tungsten segment was behind the original assembly position (Item 3);
- The external shell sabot was broken at the end of the thread (Item 4);

The following actions will help to increase the strength of sabot assembly:

1) Replace the internal sleeve and pusher plate by a one component only;
2) Replace the polycarbonate spacers by the Ultem material;
3) Put the spacer on the same component than the pusher plate for the monolithic assembly;
4) Tighten the cover in place until just a small resistance occurs.

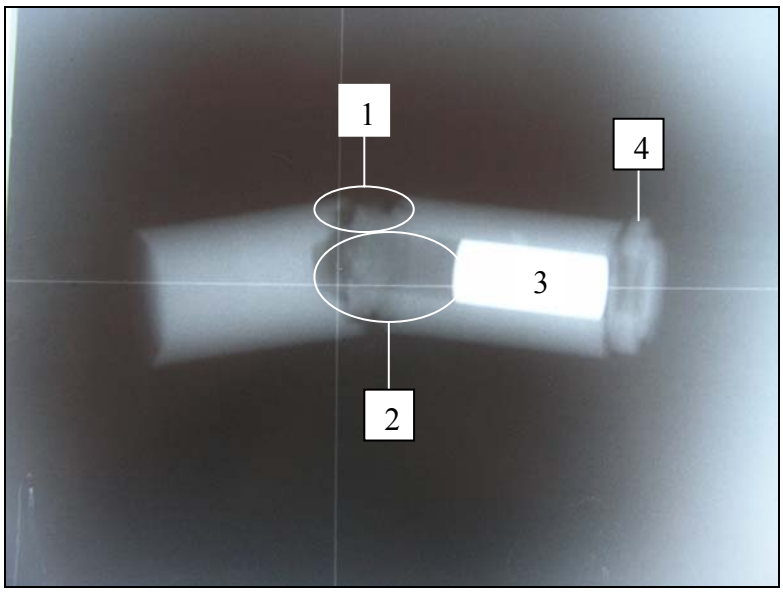

Figure 39 – X-ray of sabot in flight during the first launch

Actions 1, 2 and 3 will contribute to resolve the items 1, 2 and 3 because that reinforces the internal sleeve and fortunately the external shell at the position where the spacer is at the maximum compression. It is important to avoid as possible a joint there and an important deformation of spacers that cause a pressure in the radial direction. Action 4 will contribute to resolve item 4 by a light tightening that permits to avoid any additional stress in tension to external sleeve at the beginning of the thread.

4.2 SECOND LAUNCH CONCEPT ANALYSIS RESULTS

This section gives all the detailed results in regard with the second launch concept chosen for the preliminary sabot experimentation in the gas gun. The following sections 4.2.2 and 4.2.3 will cover results in term of analysis types. Particularly, analytic calculation as well as static numerical simulations will be covered.

4.2.1 PRESENTATION OF CONCEPT

This second launch concept is the same as concept 5, but some changes from the first launch concept have been applied. In fact, the internal sleeve and the pusher plate are now together in the same component. By now, the name pusher plate will be used to represent this new component. The term pusher plate sidewall will be used to identify especially the part in link with the internal sleeve. The second change is the replacement of the polycarbonate material spacers by the Ultem material. In addition to those modifications, this test was performed with a segmented projectile. Figure 40 shows all the components involved in the launch package for this concept. On

this figure, the white parts are in polycarbonate, the brown are in Ultem and the metallic are in tungsten. Additional pictures of this concept are available in appendix C.

Figure 40 – Components of the second launch concept assembly

Figure 41 shows the layout of the second launch concept assembly. The cyan, purple, red, blue and orange colours represent respectively the tungsten projectile, the Ultem spacers, the polycarbonate external shell, the Ultem reinforced shell and the polycarbonate cover. All the components are loaded by the front and the cover is screwed on the external shell to close the assembly. The dimensions of components are exactly the same as concept 5. Additional detailed drawings of this concept is available in appendix D.

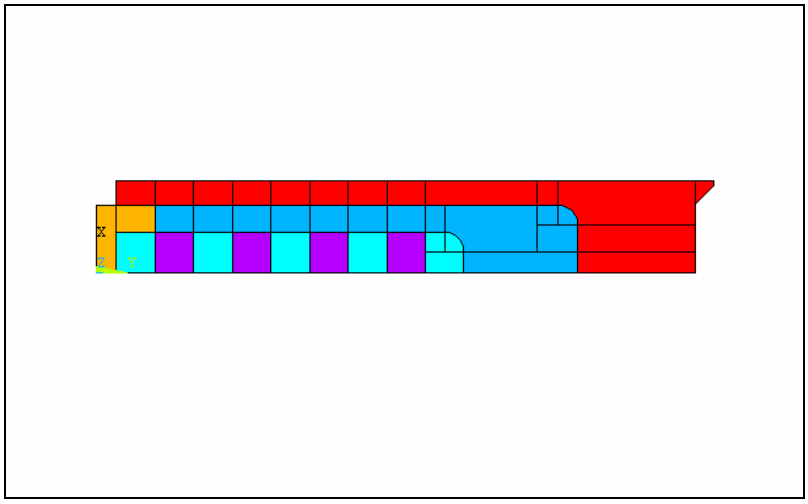

Figure 41 - Components layout for the second launch concept

4.2.2 ANALYTIC CALCULATION RESULTS

This section covers the comparison of strength for two different launch package assemblies. This comparison shows that a launch package assembly with a pusher plate and a distinct internal sleeve will respond differently in term of pressure than an assembly with a pusher plate and an internal sleeve together. The purpose of this calculation will permit to prove that the solution with the pusher plate and an internal sleeve together is stronger and offers an improvement in term of pressure compare to the solution of the launch concept 1.

To prove this aspect of comparison, the pressure of the two assemblies will be calculated in an analytic way. In fact, because the first launch concept had a joint between the internal sleeve and the pusher plate, the calculation of the maximum pressure will be done for the external shell only. This is true if we take the assumption that the joint between the internal sleeve and the pusher plate is so important that it does not contribute to the calculation of the pressure. At the opposite, the maximum pressure for launch concept 2 considers the presence of the pusher plate sidewall and the external shell in the calculation, because it has no joint on the new pusher plate. This means, the joint does not exist and to break the external shell, the pressure must break also the pusher plate sidewall.

These pressure calculation permit to evaluate the survivability of different assemblies in a launch scenario. Equation 4.1 permits to calculate the maximum pressure on the shell components assembly. The detailed calculations are available in Appendix B.

$$P = \frac{S * E * t}{Ro - 0.4 * t} \tag{4.1}$$

Where P is the pressure from the compression of the spacers
S is the ultimate strength
E is the joint efficiency (equal to 1 is this case)
t is the thickness of the studied component
Ro is the outside radius of the studied component

Table 7 shows the analytic results of pressure for the external shell alone and also for the assembly that includes the external shell and the pusher plate. The results shows that the assembly of external shell + Pusher plate is 2.2 times stronger in pressure than the external shell alone. The calculation SABOT-EC-B-01 is available in appendix B for the calculation details of the pressure resistance.

Table 7 – Admissible pressure on the shell components for the launch concept 2

Maximum pressure on the External shell only (MPa)	Maximum pressure on the External shell+ Pusher plate assembly (MPa)	Variation
22.3	71.1	219 %

Table 8 compares the maximum pressure the shell would resist and the maximum analytic pressure developed by spacers. The analytic pressure comes particularly from the side pressure of spacers when compression occurs on them. For the calculations, the spacers are assumed to be in Ultem material. The detailed calculations are available in Appendix B. The calculation SABOT-EC-B-02 is available in appendix B for the calculation details of pressure developed by spacers.

Table 8 – Pressure analytic calculation results for the launch concept 2

Components	Shell pressure resistance (MPa)	Pressure developed by spacers (MPa)	Validation
External shell only	22.3	40.7	Failed
External + reinforced shell assembly	71.1	40.7	OK

Table 8 shows that the external shell alone had no chance to survive when the spacers developed the maximum of pressure from the compression generated by the acceleration of the launch package. This point explains the failure of the external shell of the launch concept 1. In opposite, the assembly of the external shell with the pusher plate wall would resist to the same compression. This means that the pusher plate in one part increased the strength and gave more chance of success for launch concept 2 in term of analytical calculation.

4.2.3 STATIC NUMERICAL SIMULATION RESULTS

This section gives the static analysis results on the sabot assembly components such as the pusher plate and the external shell around the projectile. The results will be evaluated for the stress in x, xy and y-axis.

Figure 42 shows the pusher plate numerical simulation result for the stress in the xy-axis. A stress concentration occurred at the radius in contact with the last segment of the projectile. The maximum shear stress was around 63.5 MPa at this place. The admissible value for the Ultem is 103.4 MPa. This means the pusher plate with these dimensions and this shape would resist in shear to the launch of the front-loading segmented design. In comparison with the rear loading segmented design, the shear stress value was higher by 9.7 %.

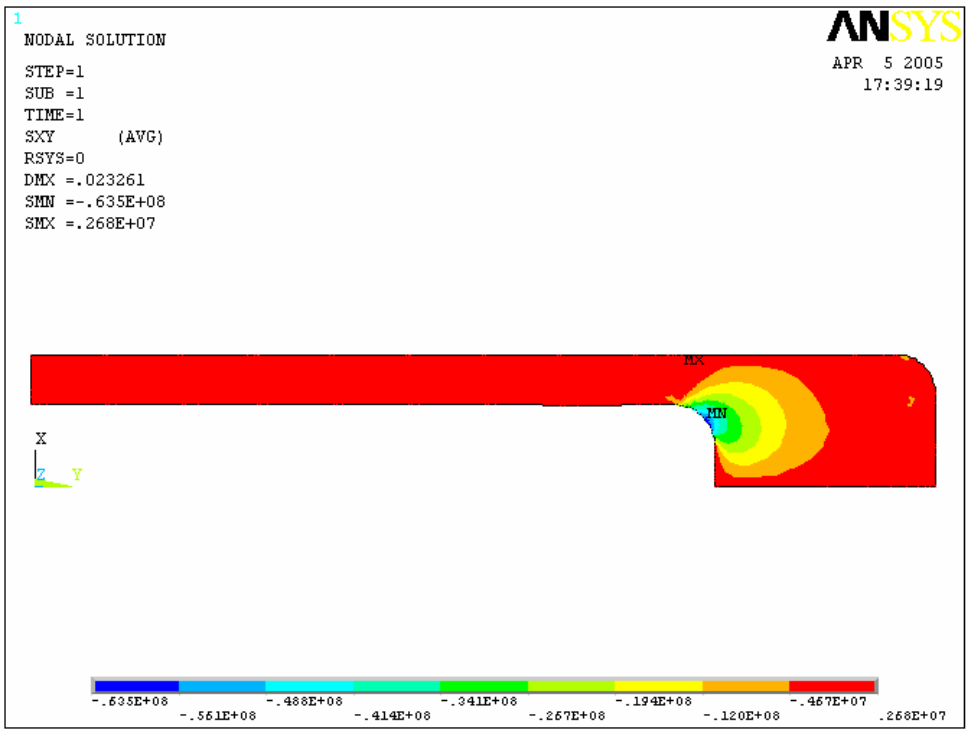

Figure 42 – Pusher plate shear stress in xy-axis for the launch concept 2

Figure 43 shows the external shell numerical simulation result for the stress in the xy-axis.

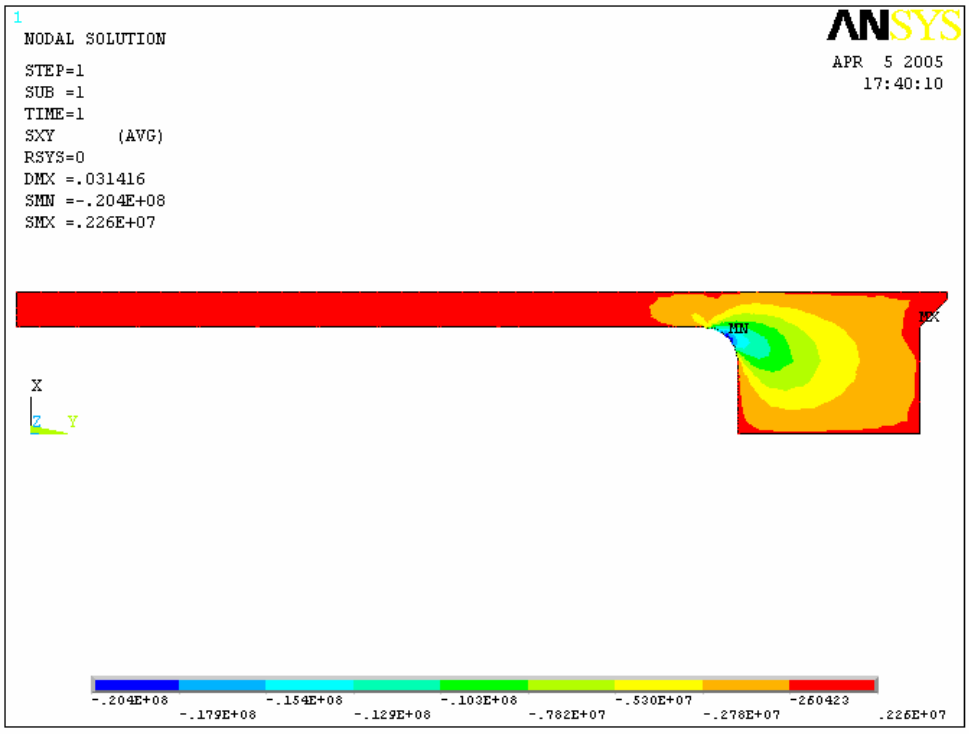

Figure 43 – External shell shear stress in xy-axis for the launch concept 2

In the previous figure, a stress concentration occurred at the radius in contact with the pusher plate. The maximum shear stress was exactly the same as for the launch concept 1 with a value of 20.4 MPa. The admissible value for the polycarbonate is 72.4 MPa. This means the external shell with these dimensions and this shape would resist in shear to the launch of the front-loading monolithic design.

Figure 44 shows the pusher plate numerical simulation result for the stress in the y-axis. On this part, a maximum compression stress occurred rear the last segment of the projectile. The maximum value was around 151 MPa. This value was under, but very close to the admissible value of 151.7 MPa for the Ultem. This means the pusher plate with these dimensions and this shape was border line in term of resistance in compression to the launch of the front-loading monolithic design. For the same reason already mentioned for the launch concept 1, the assembly will be launched and will probably success despite this high compression stress value. A maximum tensile stress of 68.9 MPa also occurred at the end of the radius in link with the sidewall part of the external shell. The value was under the admissible value of 113.4 MPa for the tensile strength of Ultem.

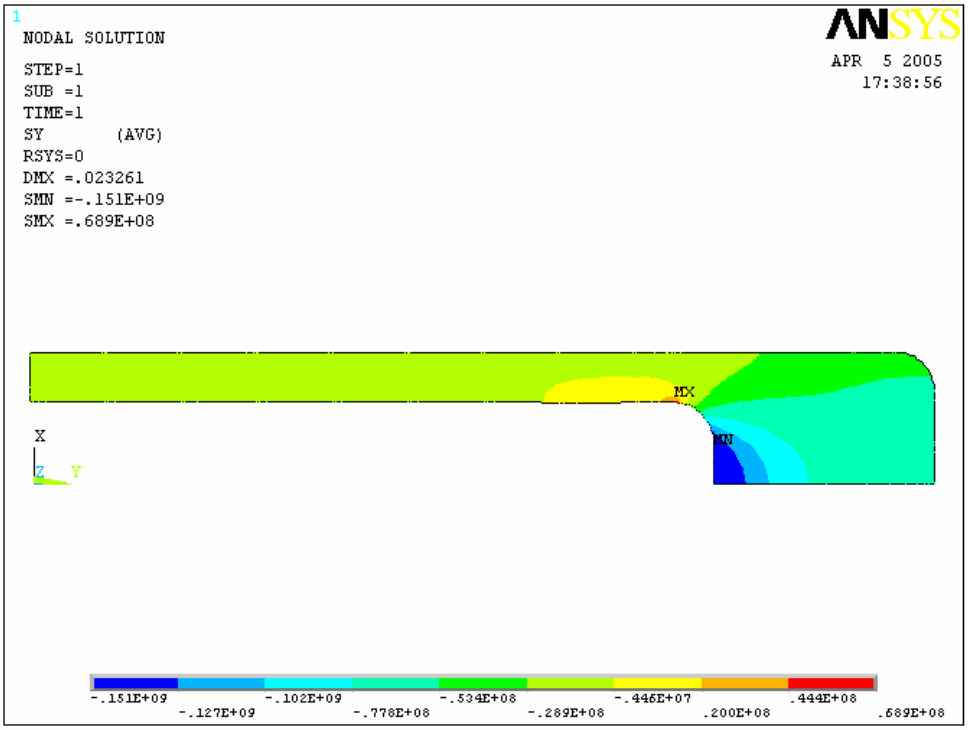

Figure 44 – Pusher plate compression stress in y-axis for the launch concept 2

Figure 45 shows the external shell numerical simulation result for the stress in the y-axis. On this part, a maximum compression stress occurred rear the pusher plate. The maximum compression stress was exactly the same as for the launch concept 1 with a value of 56.4 MPa. This value was under the admissible value of 79.9 MPa for the compressive strength of polycarbonate. Also, a maximum tensile stress occurred at the end of the radius in link with the sidewall part of the external shell.

The maximum value was around 24.3 MPa. The value was the same compared to the launch concept 1 and was under the admissible value of 72.4 MPa for the tensile strength of polycarbonate. This means, the external shell would resist tension and compression to the launch in the front-loading segmented design.

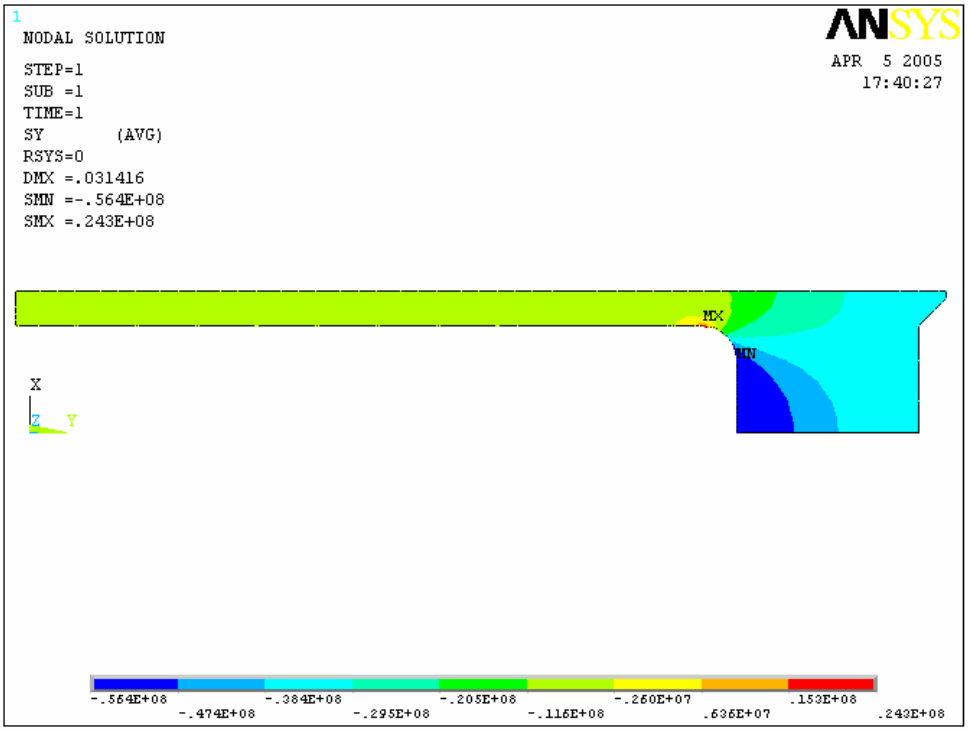

Figure 45 – External shell compression stress in y-axis for the launch concept 2

Figure 46 shows the spacer numerical simulation result for the stress in the y-axis. On this part (See black circle), a stress value of 307 MPa represented the maximum value in compression. This value was over the admissible value of 113.4 MPa for the compressive strength of Ultem. Even if the stress value in compression was higher than the admissible value it was chosen to keep the spacer in Ultem. This was decided firstly because the pusher plate without a joint will ensure a better confinement than launch concept 1 for the spacers. Secondly, the spacers are stronger and the deformation would be less important than for the previous launch concept. This launch concept represents an improvement in comparison with the last one and shows interesting things to test. This is why the launch concept 2 will be launched despite the higher stress value in compression compared to the admissible value.

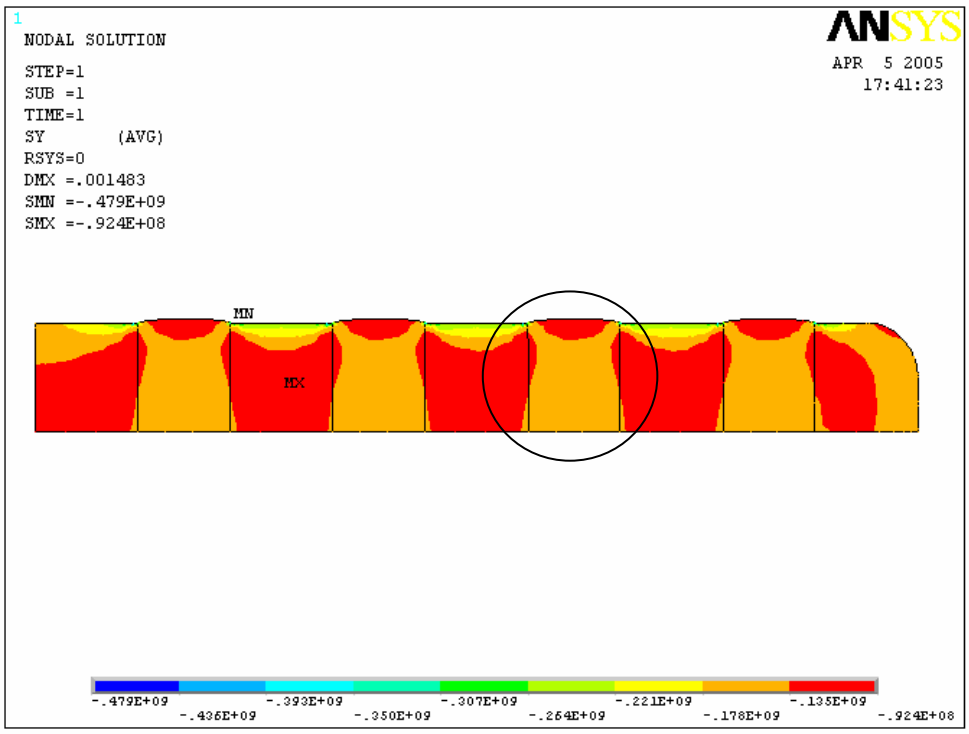

Figure 46 – Segments and spacers compression stress in y-axis for the launch concept 2

Figure 47 shows the pusher plate numerical simulation result for the stress in the x-axis.

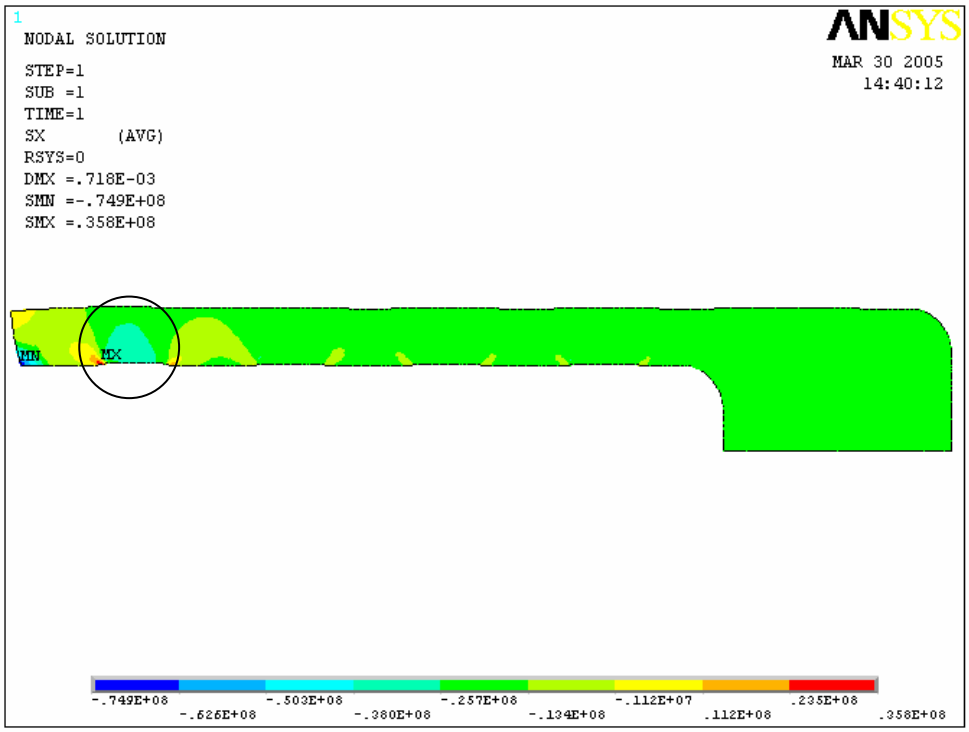

Figure 47 – Pusher plate radial stress in x-axis for the launch concept 2

In the previous figure, the simulation was done with the assumption that the sabot was still in the canon and a pressure of 200 MPa was applied to it. On the external shell, a maximum radial stress of 50.3 MPa occurred at the joint between the internal sleeve and the pusher plate. This maximum value was under the admissible stress of 113.4 MPa for the tensile strength of Ultem

4.2.4 LAUNCH RESULTS

This section shows the characteristics of the second launch package in flight and the damage the sabot suffered before it impacted the target. This concept is linked with experimentation number 18 at the hypervelocity impact laboratory. The total weight of the assembly was 697.3 grams and the total weight of tungsten was 339.05 grams.

Figure 48 shows an X-ray of the launch package in flight before it reached the target. On this figure, it is possible to see the following points:

- The segments and spacers took distance in comparison with the original position of the components (Item 1).
- The reinforced shell and the external shell took distance in comparison with the original position of components (Item 2);
- The external shell was broken at the end of the thread (Item 3);
- The cover was broken by the shear action of the projectile (Item 4).

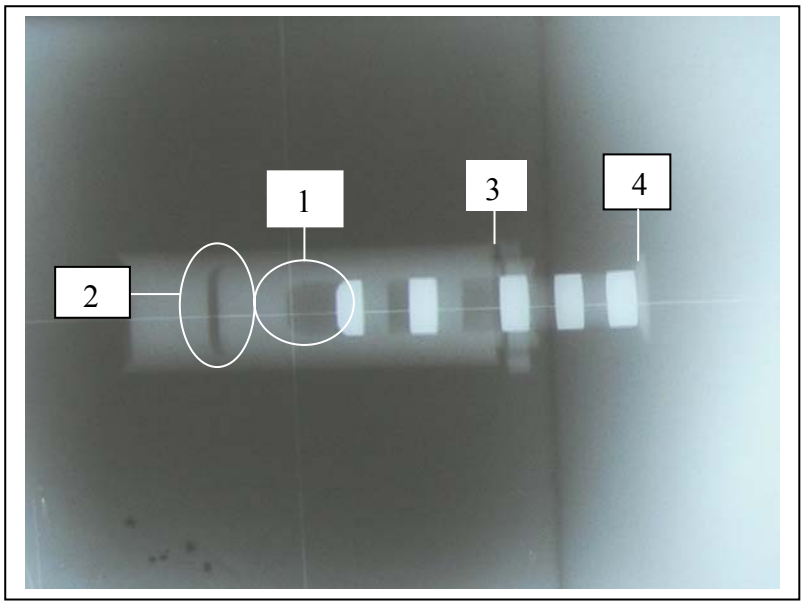

Figure 48 – X-ray of sabot in flight during the second launch

The following actions will help to increase the strength of sabot assembly:

1) Replace the thread between the external shell and the cover by bonding material. Removal of the thread will permit to reduce the change of section on the external shell and the stress concentration factor at the teeth of the thread;

2) Change the radius dimension on the segment in contact with the cover;
3) Increase the cover thickness to resist to the stress of the launch package after the acceleration stop.

Actions 1, 2 and 3 will contribute to resolve all four items listed before because they are all linked with the strength of the cover. These actions were not incorporated in the design before the fourth launch concept. This is because it was necessary to evaluate also the reinforced shell behaviour on the monolithic concept and control only a parameter per trial.

4.3 THIRD LAUNCH CONCEPT ANALYSIS RESULTS

This section gives all the detailed results in regard with the third launch concept chosen for the preliminary sabot experimentation in the gas gun. The section 4.3.2 will cover results in term of static analysis. The modifications presented in this concept should improve the strength of the launch package in comparison with the first launch concept.

4.3.1 PRESENTATION OF CONCEPT

The third launch concept is the same as the second launch concept except that it is adapted for the monolithic projectile. In fact, the internal sleeve and the pusher plate are together in the same component like for the second launch concept, but furthermore, the spacer behind the projectile is also merged with the pusher plate. This new component will keep the name of pusher plate. Figure 49 shows all the components involved in the launch package for this concept. On this figure, the white parts are in polycarbonate, the brown is in Ultem and the metallic one is in tungsten. Additional pictures of this concept are available in appendix C.

Figure 49 – Components of the third launch concept assembly

Figure 50 shows the layout of the third launch concept assembly. The cyan, red, blue and yellow colours represent respectively the tungsten projectile, the polycarbonate external shell, the Ultem pusher plate and the polycarbonate cover. All the components are loaded by the front and the cover is screwed on the external shell to close the assembly. The dimensions of the components are exactly the same as the first launch concept at the exception of the pusher plate length (L) behind the projectile with a value of 74 mm. Additional detailed drawings of this concept is available in appendix D.

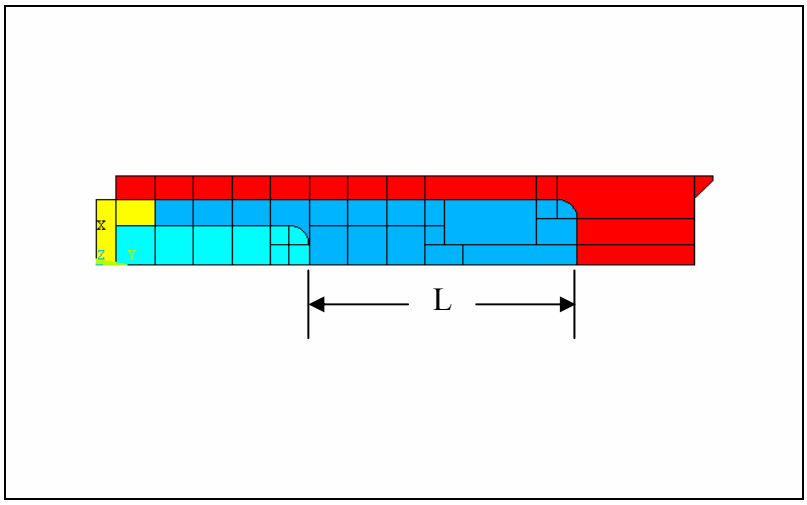

Figure 50 - Components layout for the third launch concept

4.3.2 STATIC NUMERICAL ANALYSIS RESULTS

This section gives the static analysis results on the sabot assembly components such as the pusher plate and the external shell around the projectile. The results will be evaluated for the stress in x, xy and y-axis.

Figure 51 shows the pusher plate numerical simulation result for the stress in the xy-axis. A stress concentration occurred at the radius in contact with the projectile. The maximum shear stress was almost the same as the previous design with a value of 63.9 MPa at this place. The admissible value for the Ultem is 103.4 MPa. This means the pusher plate with these dimensions and this shape would resist in shear to the launch of the front-loading segmented design.

Figure 52 shows the external shell numerical simulation result for the stress in the xy-axis. A stress concentration occurred at the radius in contact with the pusher plate. The maximum shear stress was exactly the same compared to the launch concepts 1 and 2 with a value of 20.4 MPa. The admissible value for the polycarbonate is 72.4 MPa. This means, the external shell with these dimensions and this shape would resist in shear to the launch of the front-loading monolithic design.

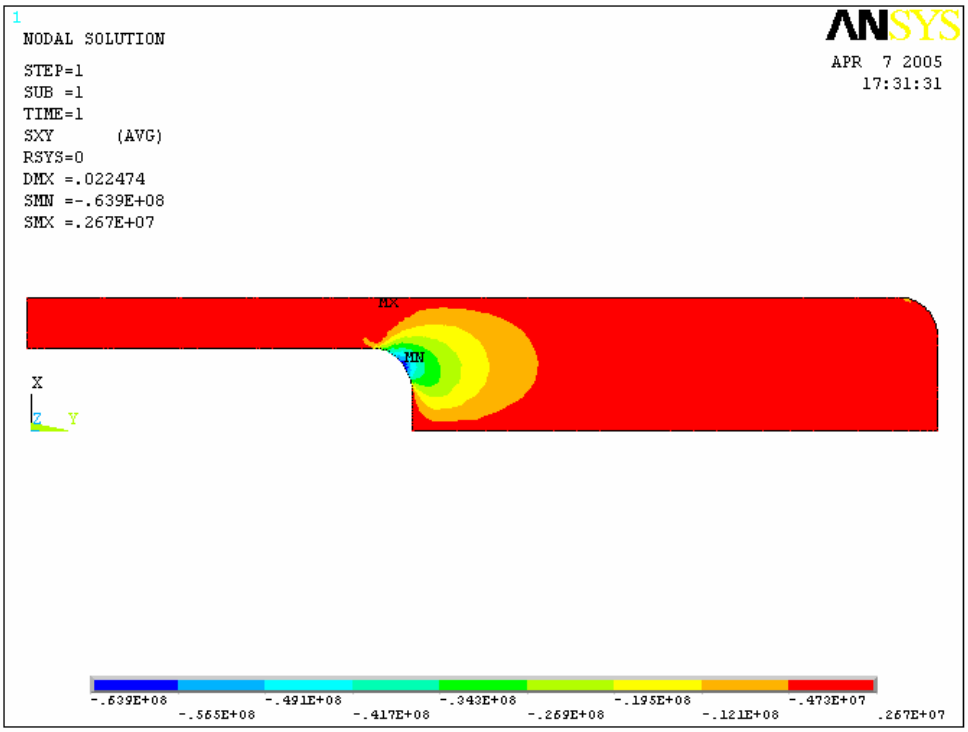

Figure 51 – Pusher plate shear stress in xy-axis for the launch concept 3

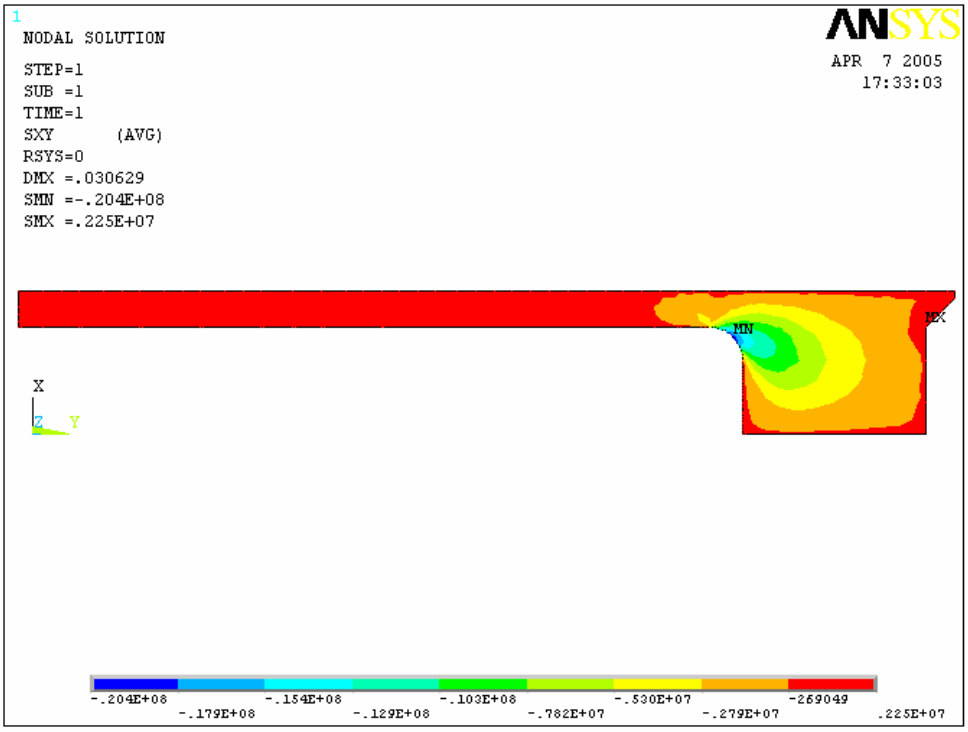

Figure 52 – External shell shear stress in xy-axis for the launch concept 3

Figure 53 shows the pusher plate numerical simulation result for the stress in the y-axis. On this part, a maximum compression stress occurred rear the projectile. The maximum value was around 151 MPa. This value was under, but very close to the admissible value of 151.7 MPa for the Ultem. This means the pusher plate with these dimensions and this shape was border line in term of resistance in compression to the launch of the front-loading monolithic design. For the same reason already mentioned for the launch concept 1 and because it had succeeded for the launch concept 2, the assembly was launched despite its high compression stress value. In tensile, the maximum tensile stress of 69.2 MPa also occurred at the end of the radius in link with the sidewall part of the external shell. The value was under the admissible value of 113.4 MPa for the tensile strength of Ultem.

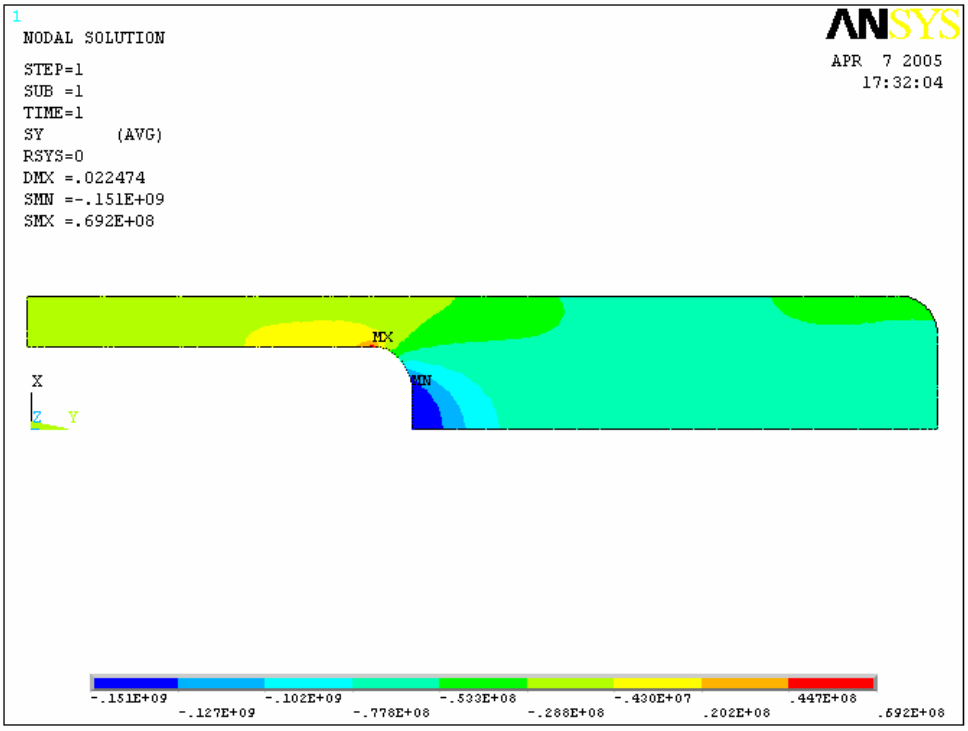

Figure 53 – Pusher plate compression stress in xy-axis for the launch concept 3

Figure 54 shows the external shell numerical simulation result for the stress in the y-axis. On this part, the maximum value in tension and compression were exactly the same compared to the concept of the two last launch concepts. In fact, the maximum compression value of 56.4 MPa was under the admissible value of 79.9 MPa for the compressive strength of polycarbonate. In tensile, the maximum value of 24.3 MPa was under the admissible value of 72.4 MPa for the tensile strength of polycarbonate. As for previous launch test, the external shell would resist in tension and in compression.

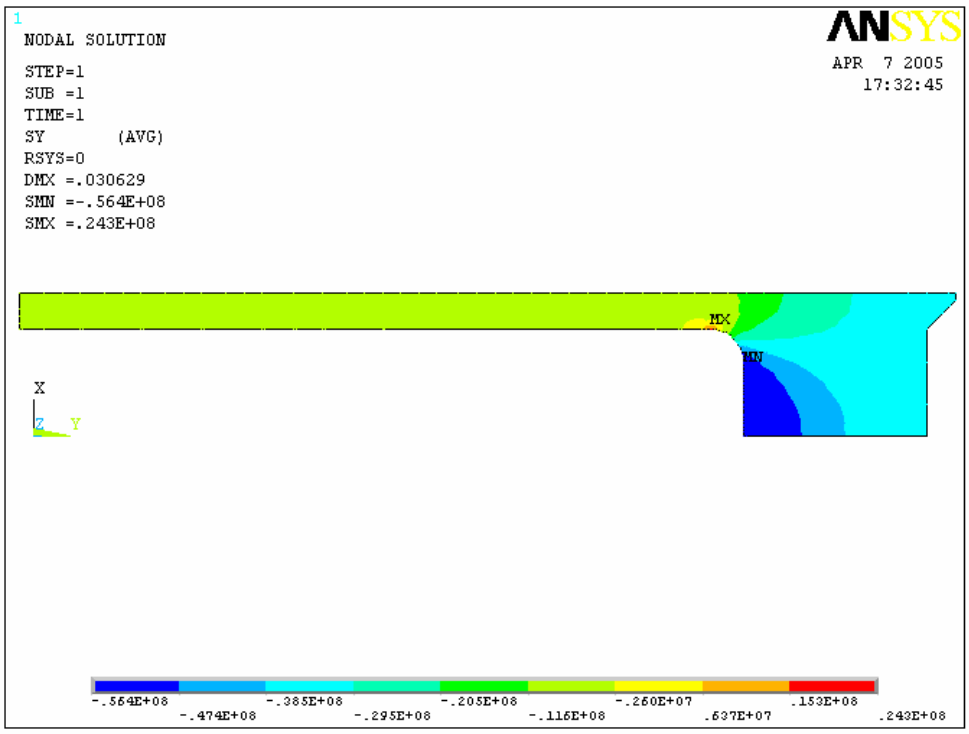

Figure 54 – External shell compression stress in xy-axis for the launch concept 3

Figure 55 shows the external shell numerical simulation result for the stress in the x-axis.

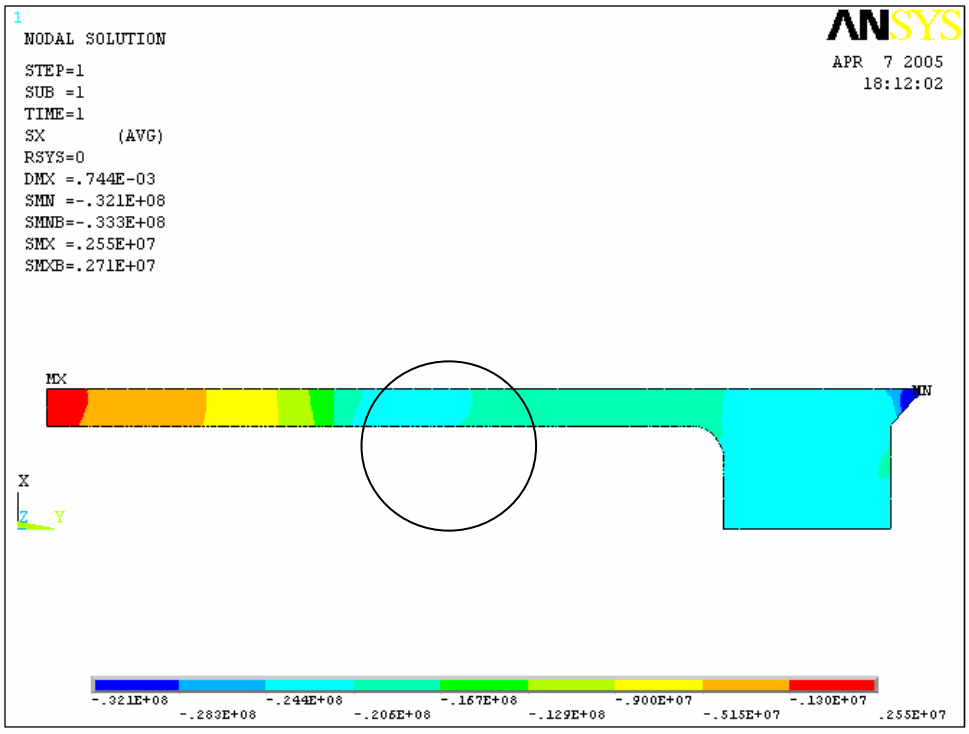

Figure 55 – External shell radial stress in x-axis for the launch concept 3

In the previous figure, the simulation was done with the assumption that the sabot was still in the canon and a pressure of 200 MPa was applied to it. On the external shell sidewall, a maximum radial stress of 24.4 MPa occurred at the section of the sabot rear the monolithic projectile (See the black circle). This maximum value was under the admissible stress of 72.4 MPa for the tensile strength of the polycarbonate.

4.3.3 LAUNCH RESULTS

This section shows the characteristics of third sabot in flight and the damage the sabot suffered before it impacted the target. This concept is linked with experimentation number 19 at the hypervelocity impact laboratory. The total weight of assembly was 696.2 grams and the total weight of tungsten was 339.36 grams.

Figure 56 shows an X-ray of the launch package in flight before it reached the target. On this figure, it is possible to see the following points:

- The projectile and the pusher plate took distance in comparison with the original position of components (Item 1).
- The pusher plate and the external shell took distance in comparison with the original position of components (Item 2);
- The external shell was broken at the end of the thread (Item 3);
- The cover was broken severely (Item 4).

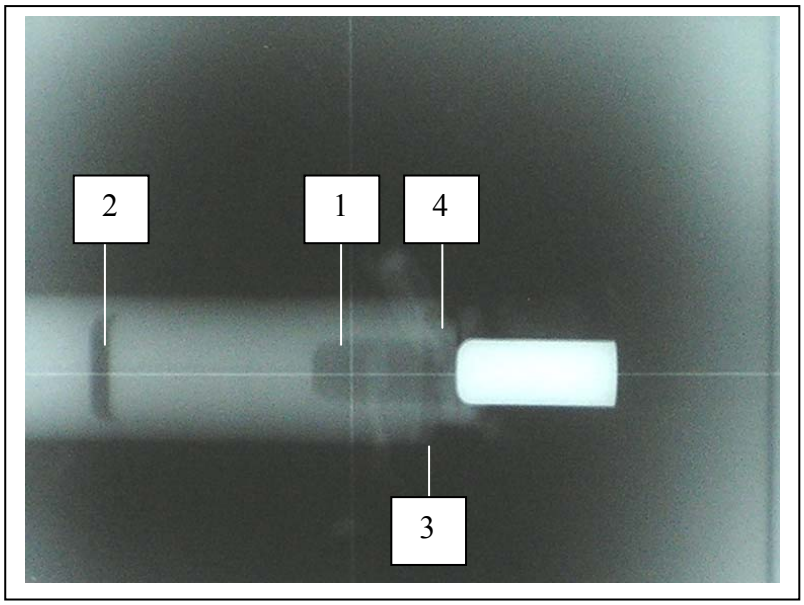

Figure 56 – X-ray of sabot in flight during the third launch

The actions to increase the strength of sabot assembly are the same than the list supplied in section 4.2.4 of the second launch concept.

4.4 FOURTH LAUNCH CONCEPT ANALYSIS RESULTS

This section gives all the detailed results in regard with the fourth launch concept chosen for the preliminary sabot experimentation in the gas gun. The following sections 4.4.2 and 4.4.3 will cover results in term of analysis types. Particularly the analysis of the analytic and static aspects will be covered.

4.4.1 PRESENTATION OF CONCEPT

The fourth launch concept is the same as the third one except for a major change on the cover already identified in section 4.2.4. In fact, the cover is ticker than before and the threads are removed. By now, the cover is bonded on the external shell with Chloroform. Also, to reduce the stress concentration on the cover, a radius is added on the front part of the tungsten projectile. Figure 57 shows all the components involved in the launch package of this concept. On this figure, it is possible to see two things: the cover has no threads on the side and the tungsten projectile has a radius on its two extremities. Additional pictures of this concept are available in appendix C.

Figure 57 – Components of the fourth launch concept assembly

Figure 58 shows the layout of the fourth launch concept assembly. The cyan, red, blue and yellow colours represent respectively the tungsten projectile, the polycarbonate external shell, the Ultem reinforced shell and the polycarbonate cover. All the components are loaded by the front and the cover is bonded on the external shell to close the assembly. Some difference appears on the dimension aspect. In fact the reinforced shell is shorter than the third launch concept with a length (L) of 100 mm. In the same way, the cover is longer and thicker than before. The cover has a thickness (t) of 25 mm. Also, the contact between the external shell and the

cover is longer than in the previous concept with a length (L2) of 25 mm. Finally, the projectile tungsten has now a radius (R) of 3 mm in the front part. Additional detailed drawings of this concept is available in appendix D.

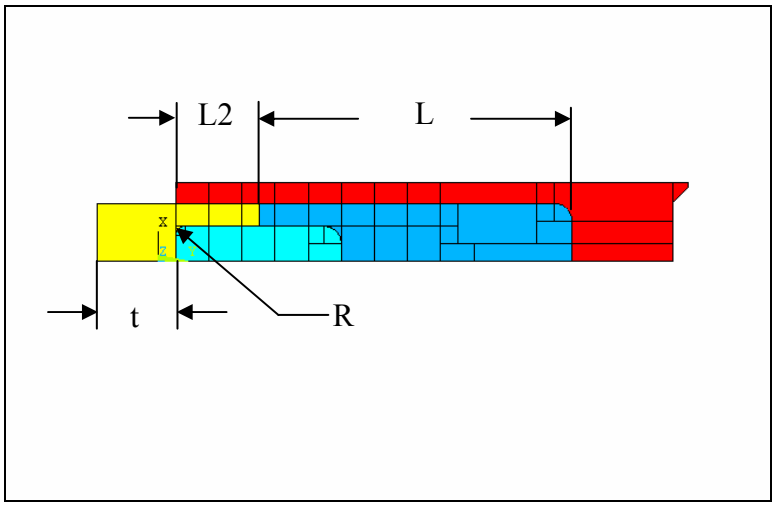

Figure 58 - Components layout for the fourth launch concept

4.4.2 ANALYTIC CALCULATION RESULTS

This section develops the front cover strength and the cover bonding strength by the analytic way. In fact, the analytic calculation establishes a force comparison to evaluate the minimum thickness of the cover and the length of the cover bonding to resist the launch package deceleration and component spring back. The spring back is caused by the liberation of the potential energy stored in the components due to elastic compression in the acceleration phase. When the projectile exits the launch tube, the acceleration is stopped and the components are then projected toward the sabot cover. The penetrator, with the spacers, impacts the cover, causing shear stress at it as well as tensile stress at the external shell in y-axis.

Equation 3.1 in section 3.1.1 is the basis of the calculation for the evaluation of the cover thickness and the bonding length with the external shell, for resistance in shear stress. For the complete evaluation of the cover thickness, the following assumptions have been used:

- All the components involved in sabot assembly are considered for the spring back
- The components are evaluated at the maximum compression value;
- All the drag and the spacer spring back energy is transferred to the tungsten projectile;
- The accepted deformation of the components during the deceleration is equivalent to the maximum deformation allowed by each material just before it failed;

- The external shell and the cover decelerate by the drag experienced in the impact chamber.

For the complete evaluation of the cover bonding length, the following assumptions have been taken into consideration.:

- Because the Chloroform permits a fusion of materials, the elongation of the bonding material is considered as the same as the cover material;
- Only 40 % of the polycarbonate strength is considered in the Chloroform bonding joint between the cover and the external shell.

The results in regards with these two last assumptions are available in table 11.

Table 9 shows the analytic results for the admissible force on the sabot in the cases with or without thread. In comparison with the maximum force applied on the sabot, this late with thread failed but it will succeed without thread. This allows to see that a sabot with appropriate bonding material would resist the maximum traction force. In this way, the bonding of the cover with the sabot is very interesting.

Table 9 – Resistance of sabot under traction force for the launch concept 4

Components	Admissible force on sabot (N)	Maximum force applied on sabot (N)	Validation
Sabot with threads	13 108	61 750	Failed
Sabot without thread	66 197	61 750	OK

The calculation SABOT-EC-E-05 is available in appendix B for the detailed calculation of the admissible force of traction on the sabot. The calculation SABOT-EC-D-08 also available in appendix B gives the detailed calculation with regards to the maximum force applied on sabot from the spring back evaluation.

Table 10 shows the analytic results to compare and evaluate the covers of generation 1 and generation 2. The cover of generation 1 is the thinner cover used for the launch concepts 1, 2 and 3. The results of admissible force for the cover generation 1 compared to the maximum force applied on the cover prove that this one was too weak. In the opposite, the cover generation 2 shows that it would resist the maximum force applied on it.

Table 10 – Resistance of cover for the spring back effect

Components	Admissible force on the cover (N)	Admissible force on threads (N)	Maximum force applied on cover (N)	Validation
Cover gen. 1	21 909	53 500	61 750	Failed
Cover gen. 2	87 638	136 600	61 750	OK

All the calculations linked with this table are available in appendix B. The detailed calculation for the admissible force on the cover generation 1 comes from the calculation SABOT-EC-D-01 while the detailed calculation for the cover generation 2 come from the calculation SABOT-EC-D-05. The detailed calculation for the admissible force on the thread of the cover generation 1 comes from the calculation SABOT-EC-D-02 while the detailed calculation for the cover generation 2 come from the calculation SABOT-EC-D-04. The calculation SABOT-EC-D-08 also available in appendix B gives the detailed calculation in regards with the maximum force applied on the cover from the spring back evaluation.

Table 11 shows the analytic results for the minimum required thickness for the cover. This table gives many thicknesses of the cover in relation with the spacer's material and the cover material.

Table 11 – Minimum front cover thickness for launch concept 4

Spacers material	Cover material	Minimum thickness
Polycarbonate	Polycarbonate	20.7 mm
Ultem	Polycarbonate	14.1 mm
Polycarbonate	Ultem	12.7 mm
Ultem	Ultem	8.6 mm

From Table 11, the assembly composed by the Ultem spacers and the polycarbonate cover was chosen for the fabrication of the fourth launch concept. The cover has a thickness of 20 mm after the fabrication because the analytic calculations propose a requirement of 14.1 mm of thickness. The choice of this combination is explained by the fact that the Ultem spacer had already prove the potential and the polycarbonate for the cover because the polycarbonate had a lower density than the Ultem and permitted to keep continuity with regards to previous launch test.

In addition to Chloroform, an acrylic bond was considered. Table 12 shows the analytic results of resistance for the Chloroform and the acrylic bonding. The comparison with the maximum force applied on the bond material allows seeing that either the Chloroform or the acrylic bonding would do the work in term of resistance. For future launch, the choice of the Chloroform is interesting because it permit a fusion between polycarbonate component rather then adding a third component as would do the acrylic bond.

Table 12 – Resistance of bond material under the spring back effect

Components	Admissible force for bond (N)	Maximum force applied on bond (N)	Validation
Chloroform bonding	71 704	61 750	OK
Acrylic bonding F246	98 960	61 750	OK

The calculation SABOT-EC-D-06 is available in appendix B for the detailed calculation of the admissible force for the bond materials. As for previous comment, the calculation SABOT-EC-D-08 is also available in appendix B and gives the detailed calculation in regards with the maximum force applied on the bond material from the spring back evaluation.

Table 13 shows the analytic results for the minimum bonding length required between the cover and the external shell. This table gives the minimum bonding length in case the Chloroform is used as the bonding material.

Table 13 – Minimum-bonding length of cover for launch concept 4

Bonding material	Minimum length of bonding	Bonding length on launch concept 4
Chloroform	21.5 mm	25 mm

Table 13 shows that the length of bonding during the assembly is 25 mm because the analytic calculations proposed a requirement of 21.5 mm of length.

4.4.3 STATIC NUMERICAL ANALYSIS RESULTS

This section gives the static analysis results on the cover components when the tungsten projectile puts a force on it. The results will be evaluated for the stress in the xy and y-axis only.

Figure 59 shows the loading and the boundary conditions on the cover for the static analysis simulation. This figure shows the same 2-dimensionnal view than figure 4 because this is an axisymmetric view. The purple part represents the front cover and the cyan part represents the tungsten projectile.

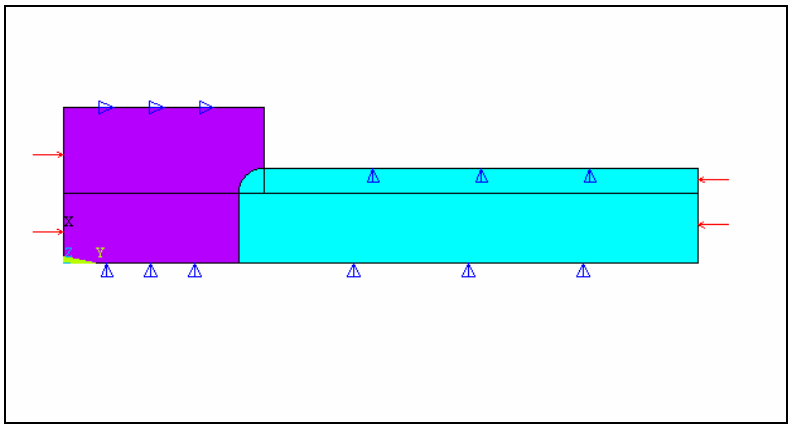

Figure 59 - Loading and boundary conditions for the static analysis of cover

The red arrows on the right represent the pressure on the projectile by the spring back effect of the spacers. This value is equal to 5.07 MPa The red arrows on the left represent the drag effect on the cover. This pressure is equivalent to 3.47 MPa. The blue triangles on the top and the bottom represent movement constraints to $\Delta x=0$ in the x-axis. The triangles on the left represent a movement constraint to $\Delta y = 0$ in the y-axis. During the simulation, the spring-back pressure minus the drag pressure pushes the projectile on the left, but the resistance comes from the locking position of the cover in the y-axis.

Table 14 gives details about the maximum stress value in the xy and y-axis for different dimensions of radius on the front cover in contact with the projectile.

Table 14 – Static stress validation on the front cover for launch concept 4

Dimensions	Type of Stress	Maximum stress (MPa)	Admissible stress (MPa)	Validation
R = 0 mm	xy	70.7	63.4	FAILED
	y	199	72.4	FAILED
R = 3 mm	xy	33.3	63.4	OK
	y	38.7	72.4	OK

Table 14 shows that a stress concentration greater than the admissible stress occurs on the cover when a radius is around 0 mm. These values were good at the condition the spacers spring back was entirely transferred to the tungsten projectile. The two first rows of table 14 are respectively showed in figures 60 and 61 while the two last rows are respectively showed in figures 62 and 63.

On figures 60 and 61, the maximum stress was exactly at the edge of the projectile. In comparison, for figure 62, the maximum stress was at the beginning of the radius while on figure 63, the maximum stress was on almost all the radius. For these figures, the area of stress is bigger, but the maximum value is lower than if no radius is involved in the design. The design of the cover with a radius of 3 mm would resist in shear and in compression at the loading applied to the launch assembly.

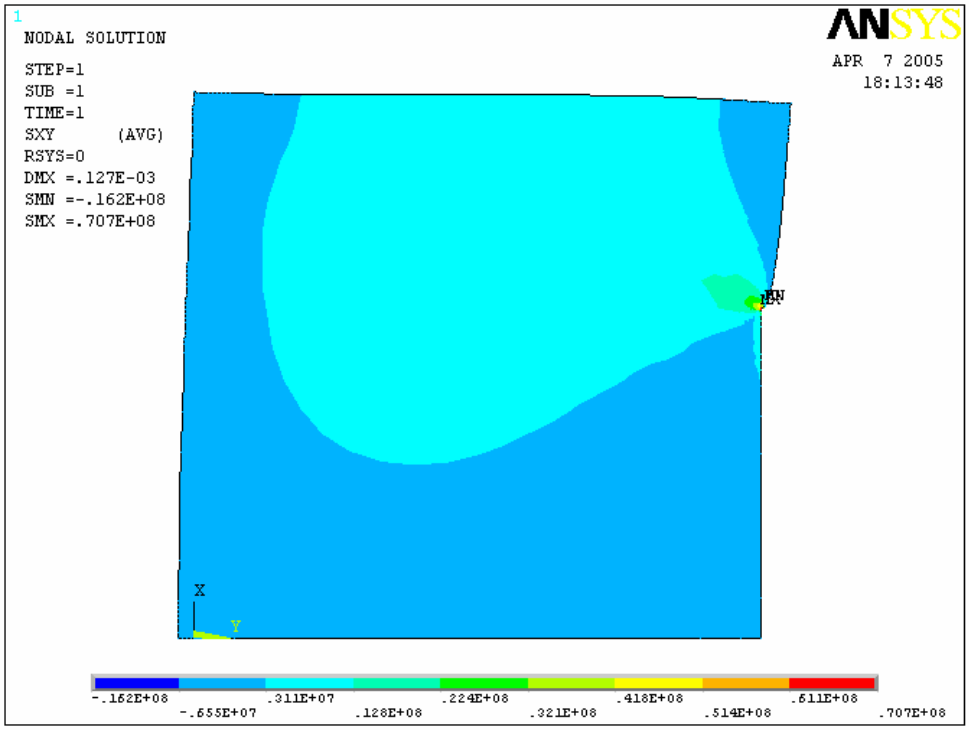

Figure 60 – Stress in xy-axis for the cover with a radius R=0 mm for the launch concept 4

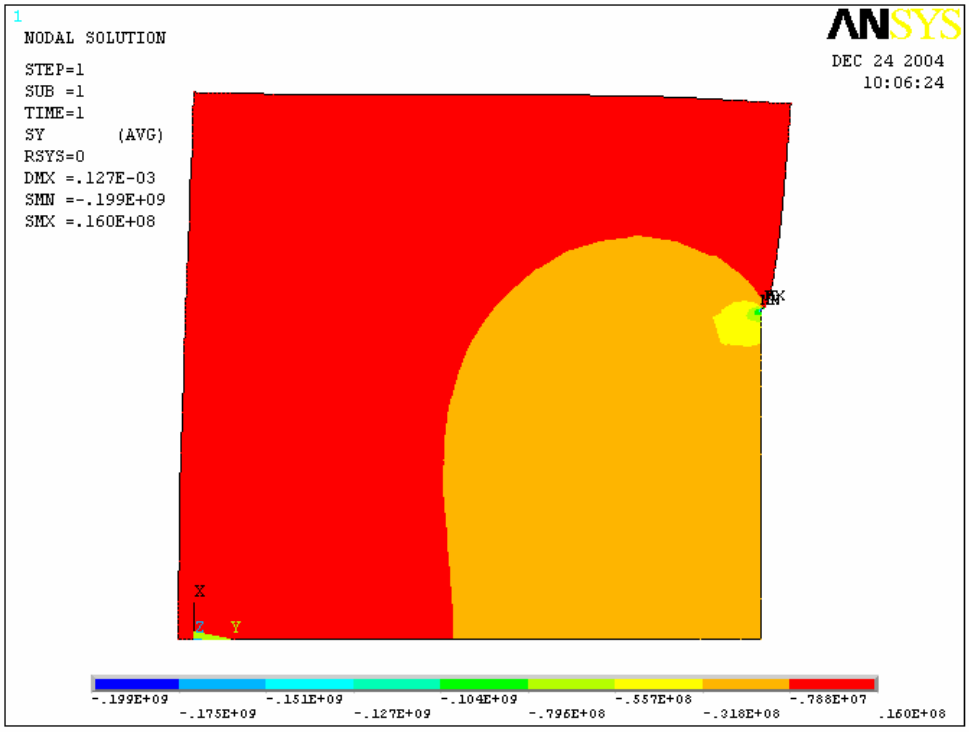

Figure 61 – Stress in y-axis for the cover with a radius R=0 mm for the launch concept 4

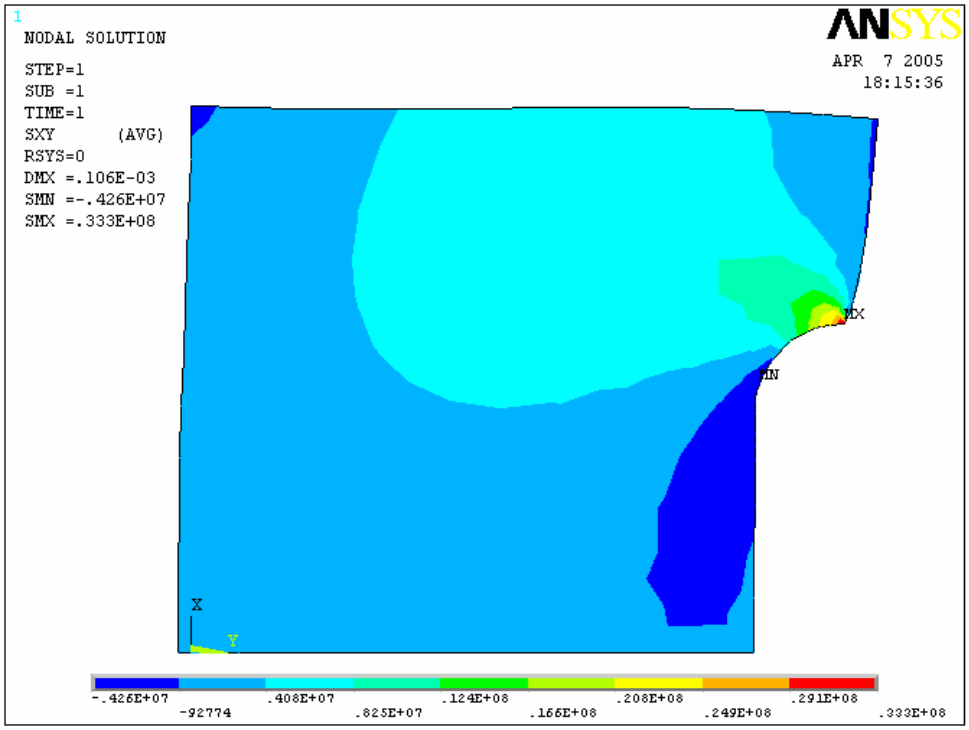

Figure 62 – Stress in xy-axis for the cover with a radius R=3 mm for the launch concept 4

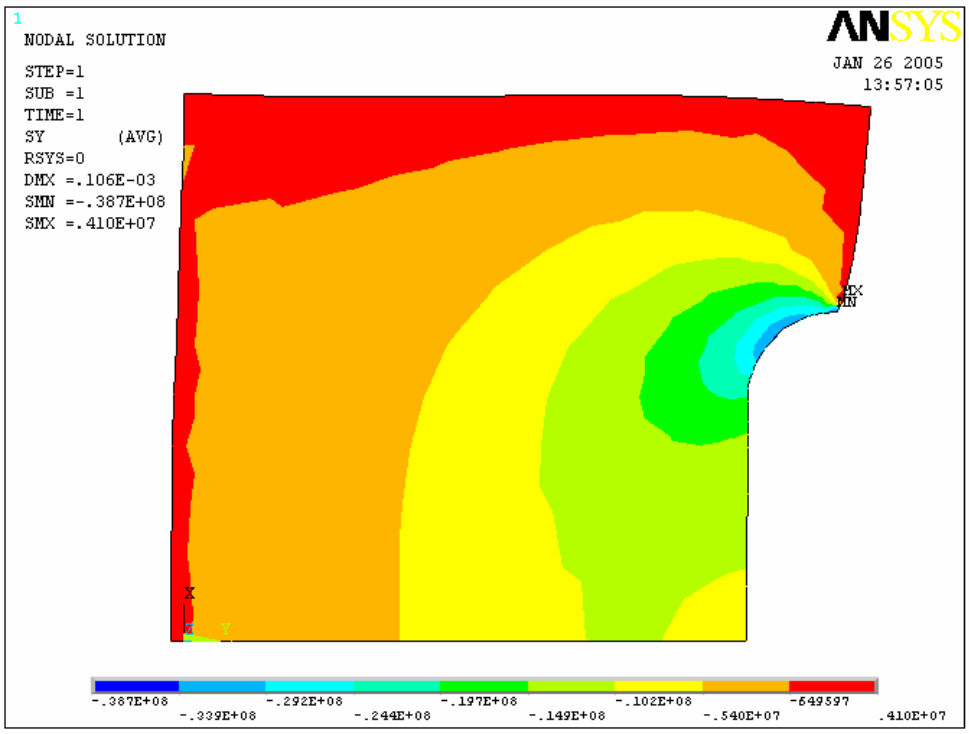

Figure 63 – Stress in y-axis for the cover with a radius R=3 mm for the launch concept 4

4.4.4 LAUNCH RESULTS

This section shows the characteristics of the fourth launch package in flight and the damage the sabot suffered before it impacted the target. This concept is linked with the experimentation number 20 at the hypervelocity impact laboratory. The total weight of assembly was 712.8 grams and the total weight of tungsten was 337.6 grams.

Figure 64 shows an X-ray of the launch package in flight before it reached the target. On this figure, it is possible to see the following points:

- The projectile and the pusher plate took distance in comparison with the original position of components (Item 1).
- The pusher plate and the external shell took distance in comparison with the original position of components (Item 2);
- The cover was separated from the external shell by the movement of the projectile (Item 3);
- The pusher plate was broken on the sidewall around the projectile. The white arrow shows where is the pusher plate material after the failure. This arrow also shows that the pusher plate sidewall is still inside the external shell. The pusher plate was failed possibly because the Chloroform decreased his strength and modified the material properties (Item 4).

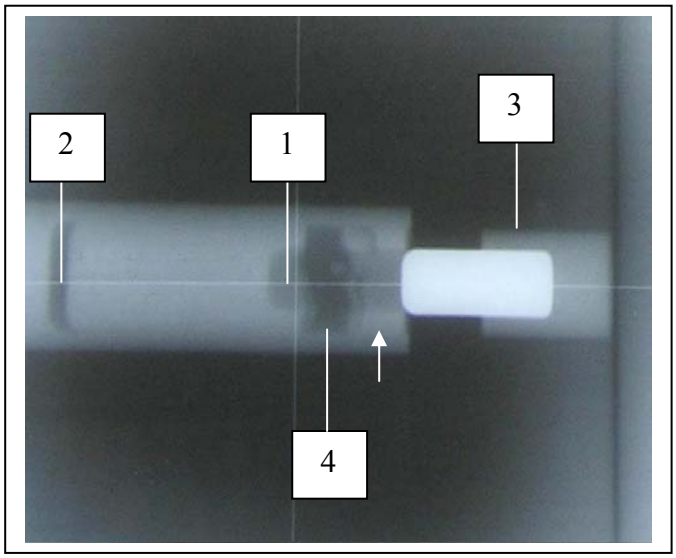

Figure 64 – X-ray of sabot in flight during the fourth launch

The following actions will help to increase the strength of the sabot assembly:

1) Evaluate the actual bonding action of the cover with the external shell;
2) Propose additional bonding material with high elongation properties;
3) Propose a bonding material that does not affect the strength of the Ultem material
4) Propose a new concept of bonding cover and external shell together.

Actions 1, 2, 3 and 4 will contribute to resolve all four items listed before because they are all linked with the bonding strength of the cover. Some trials are necessary to back-up the engineering process and propose adequate solution for the bonding aspect of the cover. These actions will not be incorporated in the design before the sixth launch concept. This mainly because it is necessary to evaluate also the cover bonding behaviour on the segmented concept and see if the bonding process would be appropriate for this concept.

4.5 FIFTH LAUNCH CONCEPT ANALYSIS RESULTS

This section gives all the detailed results with regard to the fifth launch concept chosen for the preliminary sabot experimentation in the gas gun. All analysis about the physical dimension of the cover have been done in the previous section, this one will cover the description of the concept and the launch result only.

4.5.1 PRESENTATION OF CONCEPT

The fifth launch concept is the same as the second one for what concerns the external shell, the pusher plate and the segmented projectile (segments and spacers), but is different for what concerns the cover. It includes the change on the cover presented in detail in section 4.4.1 of launch concept 4. Figure 65 shows all the components involved in the launch package for this concept.

Figure 65 – Components of the fifth launch concept assembly

At fabrication, attention was paid to avoid the contact of Chloroform with the pucher plate. It was expected to decrease the chance of having failure of the pusher plate wall as for launch concept 4.

4.5.2 LAUNCH RESULTS

This section shows the characteristics of the fifth sabot in flight and the damage the sabot suffered before it impacted the target. This concept is linked with the experimentation number 21 at the hypervelocity impact laboratory. The total weight of assembly was 713.4 grams and the total weight of tungsten was 337.0 grams.

Figure 66 shows an X-ray of the launch package in flight before it reached the target. On this figure, it is possible to see the following points:

- The segments and the pusher plate took distance in comparison with the original position of components (Item 1).
- The pusher plate and the external shell took distance in comparison with the original position of components (Item 2);
- The cover was unbound from the external shell by the movement of the projectile (Item 3);
- The surface of the second spacer and the third segment were not perpendicular to the firing line. (Item 4)

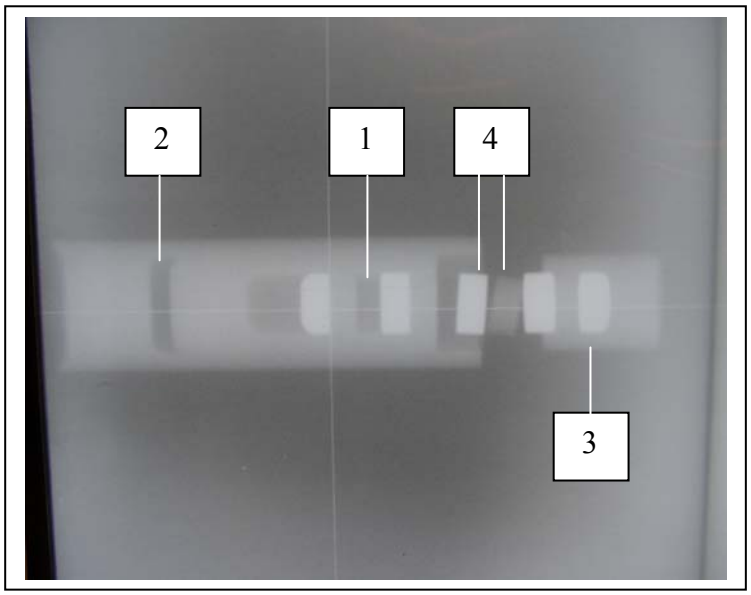

Figure 66 – X-ray of sabot in flight during the fifth launch

The actions to increase the strength of the sabot assembly are the same as listed in section 4.4.4 of the fourth launch concept, since they were implemented only for launch concept 6. It is noticeable that the pusher plate resisted the launch, meaning that it was probably the contact of the Ultem with Chloroform that caused the failure of the component for the launch concept 4.

4.6 SIXTH LAUNCH CONCEPT ANALYSIS RESULTS

This section gives all the detailed results in regard with the sixth launch concept chosen for the preliminary sabot experimentation in the gas gun. The following sections 4.6.1 to 4.6.3 will cover respectively the description of the concept, the experimentation bonding results for the cover and also the launch result.

4.6.1 PRESENTATION OF CONCEPT

The sixth launch concept is the same than the second one for what concerns the external shell, the pusher plate and the segmented projectile (segments and spacers). The cover has the same dimensions than the two previous concepts except it was not bonded on the external shell but screwed into it. The bonding process for the cover is temporally forgotten with regard to mechanical test results presented in section 4.6.2. Figure 67 shows all the components involved in the launch package for this concept. Additional pictures of this concept are available in appendix C.

Figure 67 – Components of the sixth launch concept assembly

4.6.2 MECHANICAL TESTING RESULTS OF COVER BONDING

This section shows the bench test used and the results obtained from it for different configurations of bonding application and components design. The five following sub sections present the purpose of the test, the description of the bench test, the results of trials, the analysis of results and the conclusion.

Purpose of the test

The bonding tests have been done to valid the strength of the bonding used in launch concepts 4 and 5 and at the same time explore other bonding techniques that may increase the assembly strength. Particularly, the purposes of the tests was to enough data to be able to change the design to:

- Replace the thread by an adequate bonding assembly;
- Remove or decrease significantly the stress concentration on the external shell and on the cover;
- Increase the critical section of the external shell by 14.5%;
- Find the optimal solution in term of strength for the assembly cover / external shell.

Description of bench test

Five bench tests have been tried to evaluate the capability for the cover to stay in place on the external shell when a compression force is applied to the cover. The following figure shows the link between the components. On this figure, the orange and the blue colour represent respectively the cover and the body of the external shell. The parts in grey represent the necessary components to conduct the test. The top part is the piston used to apply the force to the cover. The piston has the same dimensions than the tungsten projectile used in the sabot. The force of compression on the cover simulates the effect of projectile deceleration. The bottom part is the ring to ensure that the cover and the external shell assembly are at the good position. The tests were conducted on the Instron machine of the material characterization laboratory of the Weapons Effects Section. The force was applied to the piston until any kind of failure occurred on the assembly.

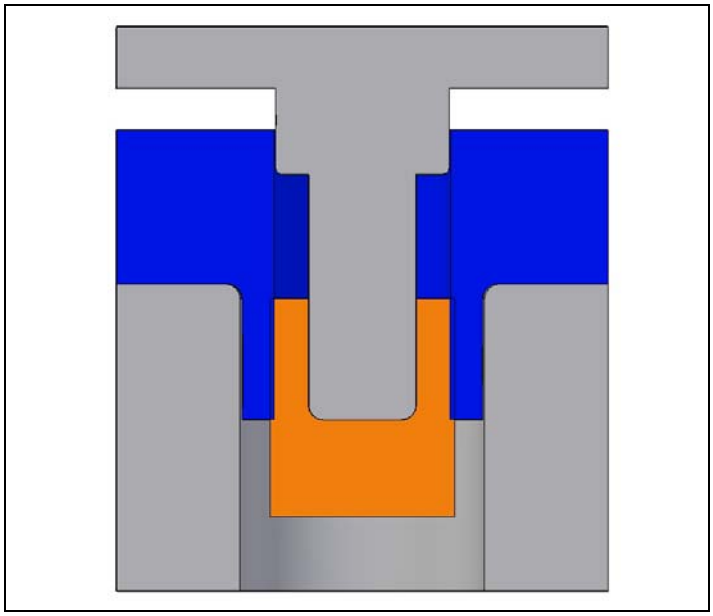

Figure 68 – Link between components for the compression test

Overall, four bench tests tried bonding application with different bonds or different bonding application process. The fifth bench test was a cover with a thread to compare this solution with the other bonding solutions. Table 15 gives some details about the tests. Figures 70 to 73 are in link with table 15 and show how the cover and the external shell were assembled.

Table 15 – Description of compression test to evaluate bonding strength

Title	Type	Characteristic	Process	Figure #
Test 1	Bonding	Chloroform	Bonding by dipping	69
Test 2	Bonding	Acrylic bond	Bonding by injection	70
Test 3	Bonding	Premixed acrylic bond	Bonding by injection	70
Test 4	Bonding	Acrylic for a flanged cover	Bonding by injection	71
Test 5	Treading	Thread 1.5-8 UNC	Cover Screwed	72

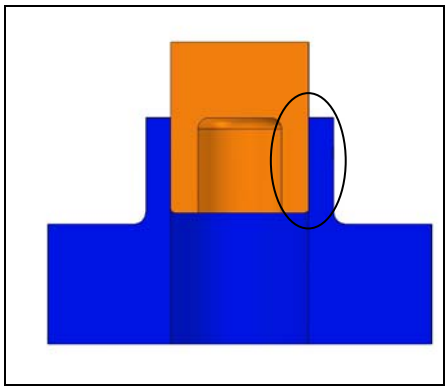

Figure 69 – Assembly for test 1

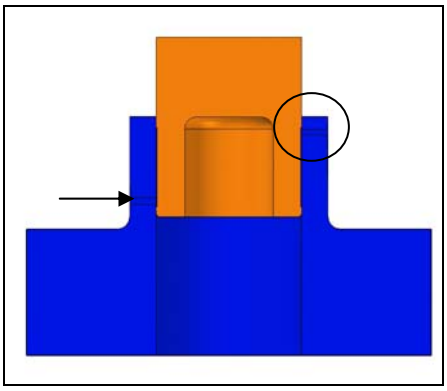

Figure 70 – Assembly for tests 2 and 3

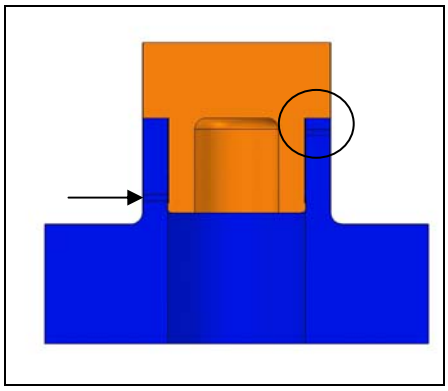

Figure 71 – Assembly for test 4

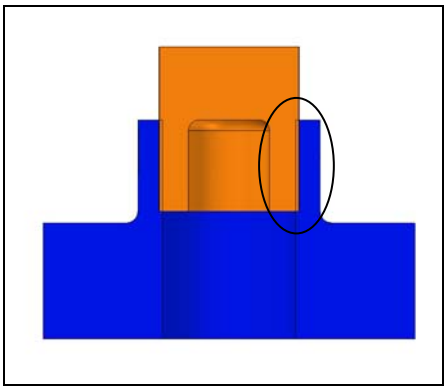

Figure 72 – Assembly for test 5

Figure 69 represents the bonding components by Chloroform for the test 1. The oval shape shows the surface of contact between the cover and the external shell. Figures 70 and 71 show by an arrow the point of injection of the acrylic and the black circle show the exit of the acrylic. A cut out on the external diameter of the cover permits to increase the thickness of the bonding. Figure 72 shows by the oval shape the surface of thread between the cover and the external shell.

Results of trials

Table 16 gives the compression test results for all assemblies presented in previous sub-section. Figure 73 shows graphically the results of the following table. The data permit to realise that the thread assembly is the stronger solution and the design with the Chloroform is the weakest solution of all.

Table 16 – Compression test results (kN) to evaluate bonding strength

	Test 1	Test 2	Test 3	Test 4	Test 5
A	24.8	17.8	20.4	20.6	39.2
B	11.7	19.1	26.6	18.6	35.5
C	9.8	17.0	18.7	25.9	35.5
Average	**15.4**	**17.9**	**21.9**	**21.7**	**36.6**

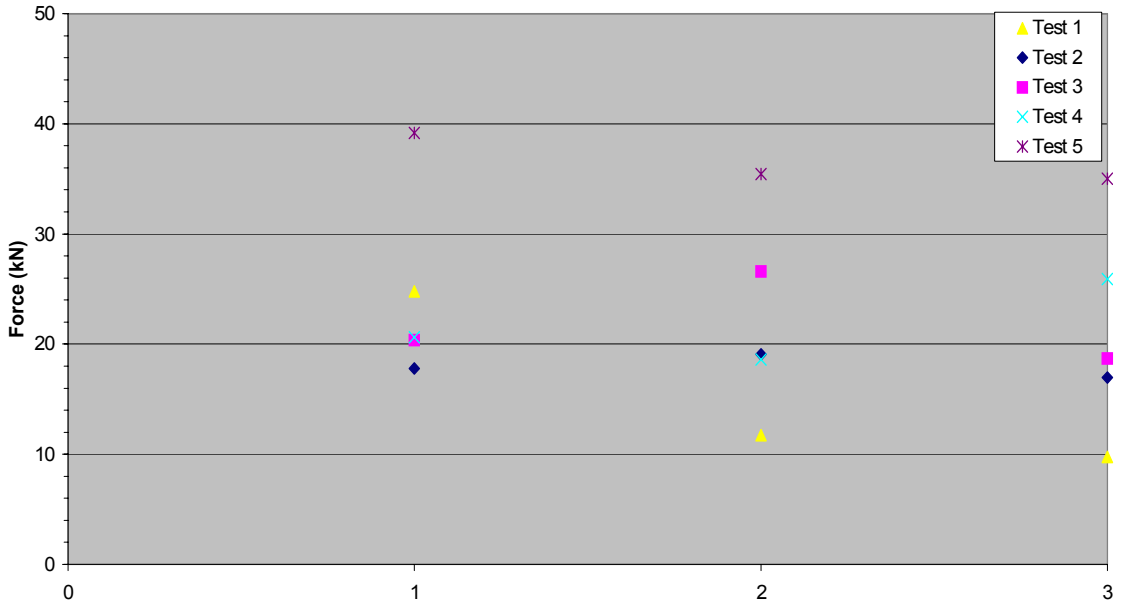

Figure 73 – Graphic of compression test results

Analysis of results

Figure 74 shows a type of failure that occurred on the assembly test 3. The results in general showed that the bonding material weakened the polycarbonate and reduced his strength in comparison with the expected result for that kind of test. In fact, for a full piece of polycarbonate without joint, the compression force to get a tensile failure should have been around 66.17 kN. This value was higher by 45 % in comparison with the average compression force on the thread (test 5) and this value was also higher by 66 % in comparison with the average compression force on the solution with an injection of a premix acrylic (test 3). Nevertheless, this solution offers the better average results for all bonding assemblies.

The maximum compression force on the thread to get a failure is lower than expected, but could be explained by the fact that in the bench test the external shell was able to move in diameter and allowed the cover to slip rather than fail under the force. During the launch test, the conditions were different and more critical because the cover left the assembly with a part of the broken external shell.

The maximum compression force on the assembly bonded with Chloroform was inadequate because this force represents only 23 % of the tensile force for the polycarbonate material. To offer the same strength than the polycarbonate, the contact between the cover and the external shell must be 4.3 times longer. This solution remains impossible on this kind of design.

The maximum compression force on the assembly bonded with an injection of acrylic offered better result compare to the solution bonded with the Chloroform. This is true in term of result, but the acrylic seemed to weaken the polycarbonate and decreased its ductility. Also, the injection needed the presence of holes that seems to increase locally the stress concentration and reduced the strength of the assembly. Figure 74 shows that the failure is close to the injection hole (The black arrow shows the hole). All the pictures of tests are available in appendix E

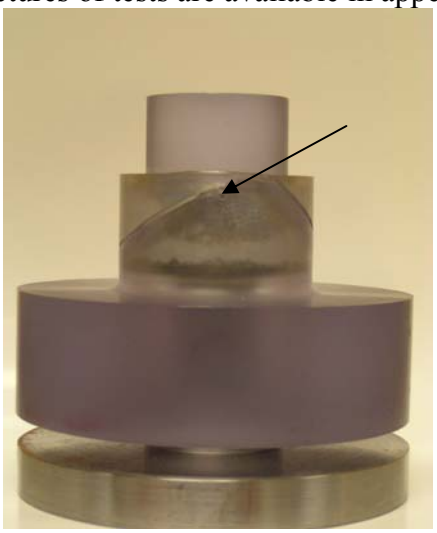

Figure 74 – Type of failure for the test 3

Conclusion

The results of tests show that the better solution for now is the assembly with a thread between the cover and the external shell. The assembly bonded with the Chloroform was not interesting because the strength value of the joint was too low in comparison with the polycarbonate material. The assembly bonded with the acrylic was also not interesting because the acrylic seemed to change the properties of polycarbonate. More, the acrylic had good bonded properties when it was injected between components. Unfortunately, the injection needed some holes that increase the stress concentration on the polycarbonate components. For those reasons, it was decided to return to threads for the assembly of launch concept 6.

If the cover and the external shell must stay together during flight, other aspects could be taken in consideration. In fact, the following points have the possibility to improve the strength of assembly:

- Replace the Chloroform or the acrylic by a more adequate bonding material such as Maxibond 9804 or Permabond E32. These bonds show better properties in term of elongation and they are not degrading the properties of polycarbonate. In fact, they are specializing for application with polycarbonate.
- Avoid any design with holes, even if they are small, to reduce stress concentration to the minimum in the component;
- Modify the shape or dimension of components to increase the section of contact between the cover and the external shell;
- Replace the actual design with a joint by an injected shell without joint. In this design, the cover and the external shell are the same piece.
- Replace the actual polycarbonate material by a stiffer one such as Ketron PEEK or Torlon. The presence of polycarbonate blade is still necessary with the use of Ketron or Torlon to protect the interior of the canon. This advice is particularly interesting for a design with a thread.

4.6.3 LAUNCH RESULTS

This section shows the characteristics of the sixth sabot in flight and the damage the sabot suffered before it impacted the target. This concept is linked with the experimentation number 22 at the hypervelocity impact laboratory. The total weight of assembly was 714.1 grams and the total weight of tungsten was 336.6 grams.

Figure 75 shows an X-ray of the launch package in flight before it reached the target. On this figure, it is possible to see the following points:

- The segments and the pusher plate took distance in comparison with the original position of components (Item 1).
- The pusher plate and the external shell took distance in comparison with the original position of components (Item 2);

- The external shell was broken at the end of the thread (Item 3);
- The surface of the third segment was not perpendicular to the firing line (Item 4);
- The flight of the external shell and the cover were not in line.

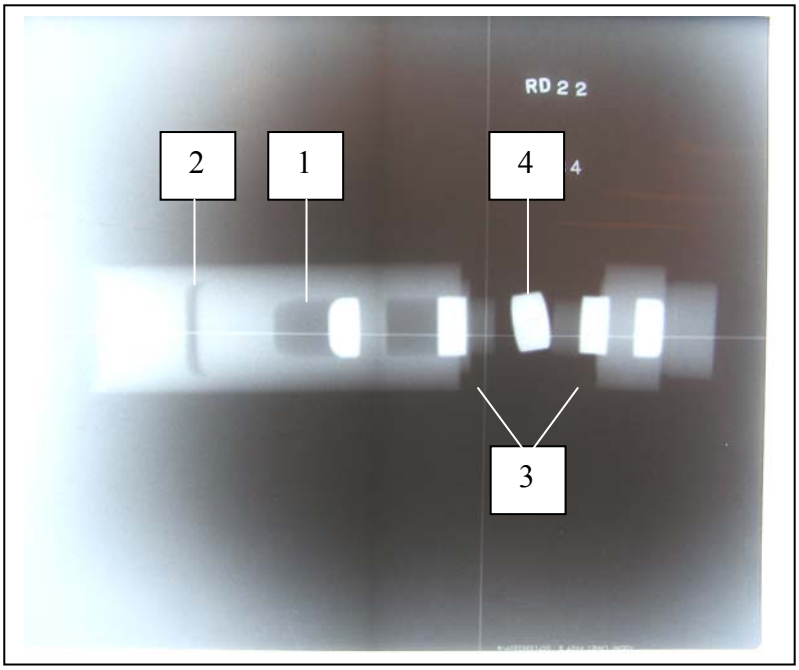

Figure 75 – X-ray of sabot in flight during the sixth launch

The following actions will help to increase the strength of the sabot assembly:

1) Add a thread between the pusher plate and the cover to keep the same distance between the cover and the pusher plate during the flight even if the external shell is broken at the end of the thread;
2) Change the material of the cover for an Ultem. This modification permits to increase the strength of the cover.

Actions 1 and 2 will contribute to resolve the items 1,2 and 4 listed before because they are linked with the thread strength of the cover. The item 3 will not be resolved because the proposed changes will not bring any additional resistance to the external shell. Until now, all the threaded covers broke the external shell at the end of the thread and liberate the projectile alone. The thread between the pusher plate and the cover is there to keep the projectile encapsulated in an Ultem shell during flight even if the external shell is broken at the end of the thread. These actions will be incorporated in the next launch concept to see if these actions could help to the survivability of the assembly.

4.7 SEVENTH LAUNCH CONCEPT ANALYSIS RESULTS

This section gives all the detailed results in regard with the seventh launch concept chosen for the preliminary sabot experimentation in the gas gun. The following

sections 4.7.1 and 4.7.2 will cover respectively the description of the concept and also the launch result.

4.7.1 PRESENTATION OF CONCEPT

The seventh launch concept introduced, as mentioned in the previous section, the design of a pusher plate with a thread and the replacement of the polycarbonate cover by a cover in Ultem material. The external shell, the pusher plate and the cover have almost the same overall dimensions than before. The only change come from the thread length on these components. Figure 76 shows all the components involved in the launch package for this concept. Additional pictures of this concept are available in appendix C.

Figure 76 – Components of the seventh launch concept assembly

4.7.2 LAUNCH RESULTS

This section shows the characteristics of the seventh sabot in flight and the damage the sabot suffered before it impacted the target. This section includes no numerical simulation because the thread was difficult to simulate and the output from this simulation did not represent a realistic results. This concept is linked with the experimentation number 23 at the hypervelocity impact laboratory. The total weight of assembly was 716.8 grams and the total weight of tungsten was 337.46 grams.

Figure 77 shows an X-ray of the launch package in flight before it reached the target. On this figure, it is possible to see the following points:

- The segments and the pusher plate took distance in comparison with the original position of components (Item 1).
- The pusher plate and the external shell took distance in comparison with the original position of components (Item 2);
- The external shell was broken at the end of the thread (Item 3);
- The pusher plate was broken at the end of the thread (Item 4);
- The penetrator took distance in comparison with the original position of components (Item 5).

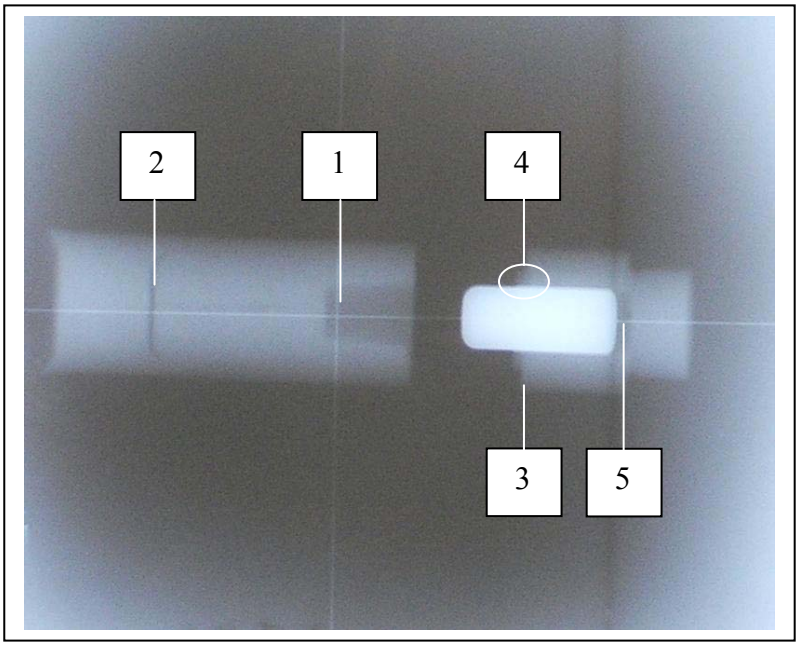

Figure 77 – X-ray of sabot in flight during the seventh launch

The following actions will help to increase the strength of the sabot assembly:

1) Change the length or the characteristics of thread along the pusher plate and the cover;
2) Evaluate the possibility of encapsulate the projectile in a shell without joint;
3) Propose a material or a mechanism able to accept by deformation the high energy of components under deceleration before they touch the cover.

Actions 1, 2 and 3 have potential to resolve all five items listed before because they are all linked with the critical points of failure during the flight. Some trials and analyses are necessary to propose an adequate solution to restrain the projectile in the shell during all the flight. These actions will not be incorporated in the design of the launch engineering concept 1 because these action are mid term solutions. This means, it is necessary to evaluate the real impact these solutions could have on the concept in term of weight, flight and also on fabrication aspects.

5.0 ENGINEERING MODEL ANALYSIS FOR EXPERIMENTATION

This section gives all the preliminary information in regard with the first launch engineering model chosen for the sabot experimentation in the gas gun. The information included in this section will stay global because a detailed description is not possible due to the confidential aspect of information in link with this part of the project. Details may be found in other reports.

5.1 SIMILARITY AND DIFFERENCE WITH THE CONCEPT DESIGN

This section gives the preliminary basis of the engineering development model in term of similarity and difference with the conceptual design.

In comparison with the conceptual design, the following points are similar to this previous concept:

- The global weight of tungsten;
- The total weight of the assembly;
- The length of tungsten segments;
- The distance between the tungsten segments;
- The layout of components in the assembly;
- Dimensions of the sabot components;
- The material composition of components in the assembly.

In comparison with the conceptual design, the following points are different :

- The weight distribution of the tungsten is divided in actual segments and retention rings;
- The spacers have different shapes and diameters;
- The diameter of the segments is smaller, but the outer diameter of the ring is the same as the conceptual segments.

5.2 POTENTIAL RING RESTRICTION METHODS

Without giving all the construction details of the engineering model penetrator, it can be mentioned that it includes two half rings to restrain the actual segments. A particular design is necessary to ensure maximum restriction strength. This section gives the preliminary possibilities to restrain rings in the engineering model. The following points give some details about the possibilities:

- Bonding the rings together by the joint: With this idea, the surface of contact for the bonding is small and the resistance of the bond will be small in the same proportion. To increase the resistance, it would be possible to bond the ring with the internal spacer;

- Adding a sleeve of aluminium or steel around the ring: The expansion of the sleeve under elevated temperature will help to introduce the sleeve around the rings. The drop of temperature will permit to keep the sleeve in place with an adequate pressure. This idea is interesting, but the sleeve cannot be thick otherwise the temperature to permit an expansion would be very important. The detailed calculation is available in appendix B;
- Adding a sleeve with a shape memory alloy: This components permits to install the same sleeve than the previous item with lower increase of temperature.
- Welding the rings together by the joint: The welding is interesting, but very expensive with a price of 500 $ per couple of ring. Also, the welding process could represent a problem for the integrity of the Ultem spacer inside the ring. If the welding is the most interesting process to restrain the ring, it could be possible to weld the ring first and inject the spacer inside the ring after;
- Adding a thinner reinforced tape around the ring couple: Some similar tests have been done on the same kind of components with standard tape that show interesting, but limited results.

6.0 IMPROVEMENT OF ACTUAL MODELS

This section gives orientations to improve the actual models in term of weight and strength. The change in term of weight will include the same type of sabot with minor changes to optimize the weight. The change in term of strength does not affect the weight, but increase the global resistance of assembly.

6.1 WEIGTH OPTIMIZATION

In this section, the following points show the items that influence the weight for a type of sabot. Every point is defined and an approximation of the removed weight is given:

- Change the front-loading by a rear loading of the projectile in the actual sabot: It is important to keep in mind that this change could bring physical modifications on the pusher plate in term of length and diameter. Particularly, the pusher plate would be longer and the diameter could be bigger to increase the shear surface between the pusher plate and the external shell. . The weight to save by this change is around 75 grams;
- Reduce the thickness of the pusher plate in the area behind the projectile: The actual thickness of the pusher plate comes from an engineering rule, which included a safety factor. In the same way, the analytical calculations and the simulations show that the thickness could be reduced. The gain of weight by this modification is around 15 grams;
- Replace the polycarbonate sidewall of the external shell for a polycarbonate blade around the Ultem pusher plate: This change allows keeping the polycarbonate in contact between the sabot and the canon to limit the canon wear, while the Ultem pusher plate keeps the projectile components together. This change reduce the weight by around 90 grams;
- Replace the Ultem material for the pusher plate component: The best candidate would by the Ketron PEEK CA30, with its better ratio strength / weight, but would save only 2 grams. Some similar analysis could be interesting with carbon fiber, but represent additional constraint on the fabrication of the pusher plate.

6.2 STRENGTH OPTIMIZATION

In this section, the following points show the items that allow a strength optimization. Every point is defined and the major advantage is identified:

- Stress relieve the polycarbonate external shell and the cover. This action would permit to decrease the stress concentration in the change of section and also reduce the possibility of micro crack;

- Add a material or a spring mechanism with a capability to take a great among of energy under deformation. This material would be between the projectile and the cover to take a maximum of energy during the deceleration phase. If the material takes a great part of the energy, for the same deformation on the cover and the external shell, the force on the polycarbonate components would be less important and the possibilities of success are very interesting. It is important to keep in mind that this material must take a great part of the energy to avoid a failure of polycarbonate components. For now no real material or spring mechanism have been identified to success in this kind of application.
- Add a system of valve inside the cover to increase the pressure inside the sabot. This idea is in the same way than the previous point. The air will take a part of the energy stocked in the projectile. The valve is simply a ball in a pipe that permit to the air to come in the cover during the acceleration time and avoid the exit of the air during the sabot deceleration time. The air trapped in the sabot would protect the polycarbonate components against failure by reducing the projectile energy. With this kind of concept, the design of the cover is more complicated and need to be stronger.

7.0 CONCLUSION

This report put some attention on the sabot resistance and on its capability to survive the loading conditions inside the light gas gun caused by the acceleration during the launch as well as the deceleration and spring back after the exit of the launch tube.

This report showed in detail the main results of the development for the sabot/projectile assembly under a pressure during the firing stage. The analytical calculation, the numerical simulations and preliminary tests have been done to support the design of the sabot at the different stages of the development.

The process of development allowed freezing definitely the design in term of material and dimension for the pusher plate, the external shell and the spacer of the projectile. These components were adequate for the monolithic, the segmented and the engineering design. Even so certain aspects of the conception work, the restraint of the cover with the external shell failed on all launch tests conducted. Some strength improvements ways were identified in the report to resolve a part of this problem. In the same way, many weight optimization points were presented in the report to give further possibilities of weight improvement for the actual sabot.

To improve considerably the performances of the projectile design, it would be interesting to change by some important ways the type of concept for the sabot, which carry the projectile. The following points define a list of possible future designs to improve some part of the results got from the launch tests.

Discarding Sabot
This concept of sabot permits to the projectile to be separated from the sabot before it reaches the target. This can be done aerodynamically or with a sabot trap. Considering the short distance from the gun exit to the target, the second one is more realistic. With this concept, the most interesting aspect is the fact that only the weight of the projectile influences the penetration on the target. In opposite, the appropriate timing of opening and the short distance to reach the target are challenging this concept.

Injection of the sabot
This concept of sabot permits to recover all the interior projectile components without any joint. With this concept, the problem of failure at the joint between the cover and the external shell disappear . However, sabot injection means that the target would be still touched by the tungsten projectile and the sabot at the same moment. To go in this way, some preliminary checks about the strength properties of moulded plastic are necessary. The injected sabot for a concept with 5 segments is possible, but limited with the actual machinery of the prototype

group. A design with more than 5 segments is impossible for now with the same machinery.

Sabot cut in two parts

This concept is similar to the discarding sabot, but the joints on the longitudinal side are bonded. A pusher plate without joint behind the projectile ensure to push the sabot in the canon. This concept is interesting because the problem of failure at the joint between the cover and the external shell do not exist because there is no joint in the circumference axis. Nevertheless, as for the injected sabot, the target would be touched by the tungsten projectile and the sabot at the same moment. Also, a sabot with a bonded joint presents some risks, the area for the bonding must be very large and the bond must have an important strength to resist the lateral stress at acceleration and the drag after launch.

8.0 APPENDIX

A – COMPLETE MATERIAL PROPERTIES X
B – COMPLETE ENGINEERING CALCULATIONS X
C – COMPLETE PICTURES OF LAUNCH CONCEPT
D - LAUNCH CONCEPT DRAWINGS
E – COMPLETE PICTURES OF BONDING TEST X